International Journal of Earth Sciences (2020) 109:1897–1920
https://doi.org/10.1007/s00531-020-01879-9

ORIGINAL PAPER

Tectonic controls on late Cambrian-Early Ordovician deposition in Cordillera oriental (Northwest Argentina)

Romain Vaucher[1,2,3] · N. Emilio Vaccari[1,2] · Diego Balseiro[1,2] · Diego F. Muñoz[1,2] · Antoine Dillinger[3] · Beatriz G. Waisfeld[1,2] · Luis A. Buatois[4]

Received: 2 August 2019 / Accepted: 14 May 2020 / Published online: 29 May 2020

Abstract

The western Gondwana margin underwent a complex geodynamic history during the early Paleozoic, and major uncertainties remain as to the role of tectonism in sedimentary dynamics. This study focuses on the lower part Santa Rosita Formation and the coeval Guayoc Chico Group (Cordillera Oriental; Northwest Argentina), ranging from the late Cambrian (Furongian; Age 10) to Early Ordovician (early Tremadocian; Tr1). This stratigraphic interval has been previously interpreted as deposited in an extensional basin to a retro-arc basin without major regional tectonic-induced deformation during its deposition, only recording long-term relative sea-level fluctuations. Four areas (Sierra de Cajas, Angosto del Moreno, Quebrada de Trancas, and Quebrada de Moya) were chosen because they host the most complete and temporally well-constrained stratigraphic sections of the Cordillera Oriental. Throughout the stratigraphic sections, four main facies zones are described and attributed to deposition in estuarine, foreshore-shoreface, delta-front, and offshore environments. Trilobite biozones are used as the biostratigraphic framework. By integrating sedimentary facies analysis, biostratigraphy, and sequence stratigraphy from the four selected sections, a new scenario showcasing the evolution of the basin is proposed. This scenario interprets a tectonically induced deformation during the deposition of the Santa Rosita Formation and the coeval Guayoc Chico Group. The newly acquired sedimentological data show that physiographical changes took place during the Cambrian-Ordovician transition and are expressed in various localities. This major change is recorded in the stratigraphic architecture, where extensive wave-ravinement surfaces and sedimentary hiatus are the result of local, syn-depositional basement uplifts. The initiation of the Puna-Famatinian volcanic arc during the Early Ordovician on the western margin was likely responsible for deformation in the retro-arc basin and the proposed scenario is consistent with the stratigraphic evolution in other areas of the Cordillera Oriental (e.g., Sierra de Mojotoro) and the Sierra de Famatina. Therefore, this study helps to constrain the evolution of the western Gondwana margin during the early Paleozoic, showing changes in the stratigraphic architecture and basin evolution from an extensional to a retro-arc style.

Keywords Retro-arc basin · Shallow-marine · Santa rosita formation · Guayoc chico group · Basin evolution

✉ Romain Vaucher
romain.vaucher88@gmail.com

N. Emilio Vaccari
evaccari@unc.edu.ar

Diego Balseiro
d.balseiro@conicet.gov.ar

Diego F. Muñoz
df.munoz@unc.edu.ar

Antoine Dillinger
antoine_dillinger@sfu.ca

Beatriz G. Waisfeld
bwaisfeld@unc.edu.ar

Luis A. Buatois
luis.buatois@usask.ca

[1] Facultad de Ciencias Exactas, Universidad Nacional de Córdoba, Físicas y Naturales. Av. Vélez Sársfield 299, X5000JJC Córdoba, Argentina

[2] Consejo Nacional de Investigaciones Científicas y Tecnológicas (CONICET), Centro de Investigaciones en Ciencias de la Tierra, (CICTERRA), Ciudad Universitaria, Av. Vélez Sársfield 1611, Edificio CICTERRA, X5016CGA Córdoba, Argentina

[3] Applied Research in Ichnology and Sedimentology (ARISE) Group, Department of Earth Sciences, Simon Fraser University, Burnaby, BC V5A 1S6, Canada

[4] Department of Geological Sciences, University of Saskatchewan, 114 Science Place, Saskatoon, SK, Canada

Introduction

Sedimentary basin evolution provides crucial information to decipher past geodynamic constraints. The Ediacaran—Early Paleozoic proto-Pacific margin of Gondwana (sensu Pankhurst and Rapela 1998) has a complex geodynamic history affected by various compressive, extensive and transpressive phases (e.g., Bahlburg and Moya 1994; Mon and Salfity 1995; Bahlburg and Hervé 1997; Dalziel 1997; Bock et al. 2000; Zimmermann and Bahlburg 2003; Bahlburg et al. 2009; Casquet et al. 2012; Zimmermann et al. 2014; Ramos 2018). The upper Cambrian (Furongian—Stage 10) to Lower Ordovician (Tremadocian—Tr1) strata of the Cordillera Oriental were deposited along the previously mentioned margin under shallow-marine to locally fluvial conditions. Nowadays, theses strata crop out extensively in northwest Argentina (Provinces of Salta and Jujuy; Figs. 1 and 2). These stratigraphic units were subject to intense paleontological (e.g., Harrington and Leanza 1957; Tortello et al. 1999; Benedetto and Carrasco 2002; Tortello and Esteban 2003; Vaccari et al. 2004; 2010; Balseiro et al. 2011; Balseiro and Waisfeld 2013; Albanesi et al. 2015; Muñoz and Benedetto 2016; Waisfeld and Balseiro 2016; Aris et al. 2017; Meroi Arcerito et al. 2018; Muñoz et al. 2018; Salas et al. 2018; Serra et al. 2019), paleoenvironmental (e.g., Moya 1988; 1998; Astini 2003; Buatois and Mángano 2003; Tortello and Esteban 2003; Buatois et al. 2006; Duperron and Scasso 2020), and sequence stratigraphic studies (Astini 2003; Buatois and Mángano 2003; Buatois et al. 2006) during the last decades. In addition, some studies focused on regional tectonostratigraphic reconstructions

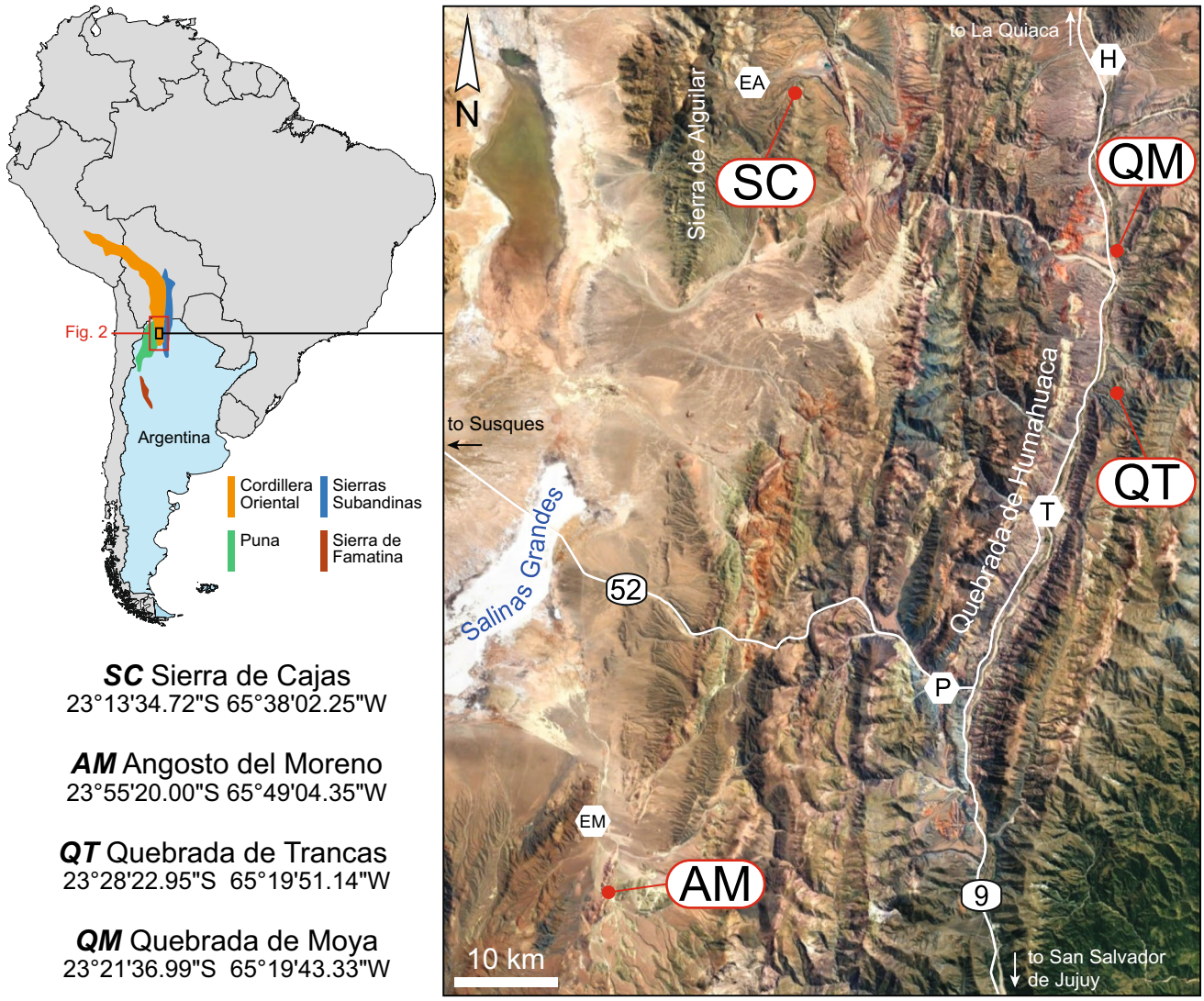

Fig. 1 Map of the studied area in the northwest of Argentina (Province of Jujuy). Satellite picture from Google Earth ©. P, Purmamarca; T, Tilcara; H, Humahuaca; EA, El Aguilar; EM, El Moreno

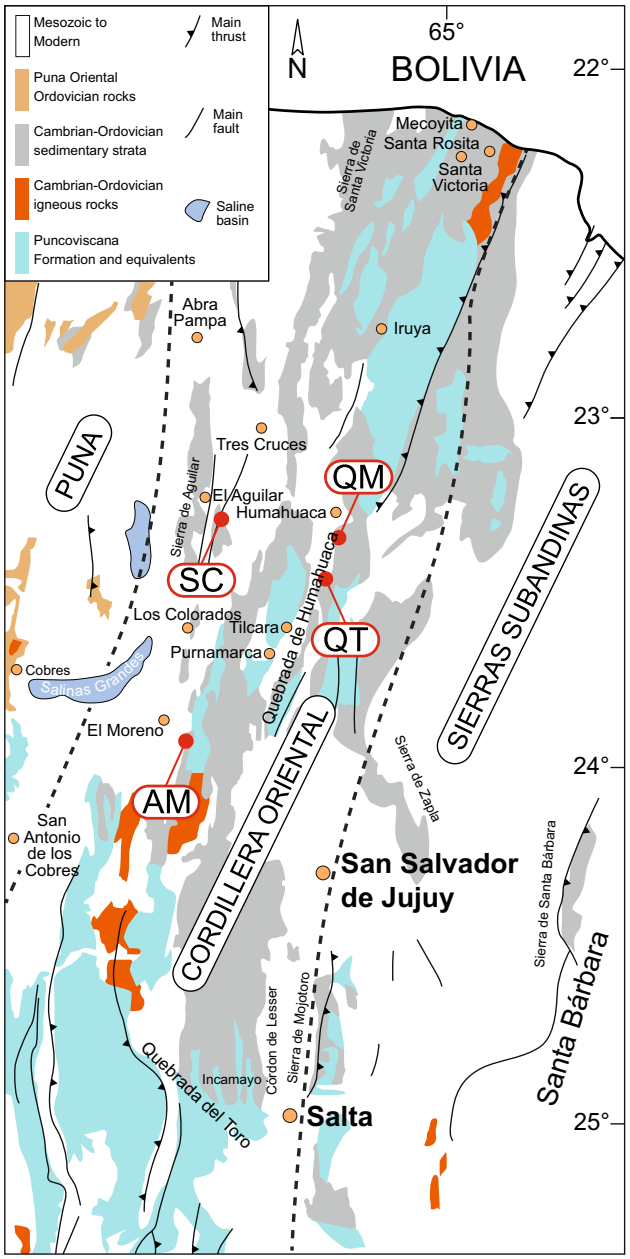

Fig. 2 Simplified geological map showing the main lower Paleozoic units cropping out in the northwest of Argentina. The name of the localities mentioned in that study are also shown. Modified after Astini (2003). SC, Sierra de Cajas; AM, Angosto del Moreno; QT, Quebrada de Trancas; QM, Quebrada de Moya

(e.g., Gohrbandt 1992; Bahlburg and Moya 1994; Bahlburg and Furlong 1996; Bahlburg and Hervé 1997; Ramos 2018). However, there is a marked paucity of studies that attempted detailed facies characterization within the context of basin evolution (Astini 2003, 2008; Egenhoff 2007).

During the late Cambrian, an extensional phase started in the basin, leading to northward widening, as well as deposition of a thicker and more extensive succession in the northern part of the basin in Bolivia (Gohrbandt 1992; Egenhoff 2007). Around the Cambrian-Ordovician transition, the onset of a subduction zone on the western border of the basin led to the development of the Puna-Famatinian arc in the Puna and Famatina areas (Figs. 1 and 2; Clemens 1993; Mannheim 1993; Mángano and Buatois 1996, 1997; Zimmermann and Bahlburg 2003; Kleine et al. 2004; Zimmermann et al. 2010; Niemeyer et al. 2018). The Furongian—lower Tremadocian Santa Rosita Formation and coeval Guayoc Chico Group were previously considered as sedimentary successions affected by relative sea-level fluctuations (Moya 1988; Astini 2003; Buatois and Mángano 2003; Buatois et al. 2006). However, Bahlburg and Hervé (1997) expected significant tectonic disturbance related to the active geodynamic context in the Puna and Famatina areas. Shortening has been estimated around 45–70 km for this area (Kley et al. 1999), although deformation associated with the development of a continental arc could occur hundreds of kilometers within the retro-arc basin (e.g., Jordan 1995).

The lower part of the Santa Rosita Formation and the coeval Guayoc Chico Group represent the focus of this study. The stratigraphic sections used herein were chosen because of (1) their exceptional vertical and lateral continuity; and (2) the highly fossiliferous content, which allowed accurate stratal correlation. This study provides new data aiming to propose an integrative and detailed reconstruction of the initiation and evolution of the Furongian—early Tremadocian at the Cordillera Oriental (Province of Jujuy; Argentina). This work combines facies analysis, biostratigraphy, and sequence stratigraphy to provide a conceptual framework of the evolution of an active margin. This contribution shows (1) previously unrecognized tectonic uplifts that occurred during the Cambrian-Ordovician transition, related to the emplacement of the volcanic arc to the west; and (2) the evolution of the basin from an extensional to a retro-arc style. Therefore, these data are not only important for the reconstruction of the studied basin but also provide new evidence helping to refine the geodynamic evolution of the western margin of Gondwana, while suggesting future research areas.

Stratigraphic nomenclature update

Cambrian (Stage 10)—Ordovician (Tr1) sedimentary successions exhibit a complex nomenclature made of formal and informal formation names that have been employed among different localities across the basin (Astini 2003 and references therein). Buatois et al. (2006) refined the stratigraphic framework of the Santa Rosita Formation for the Quebrada de Humahuaca area (east of Cordillera Oriental; Fig. 2) based on an integrated sedimentologic,

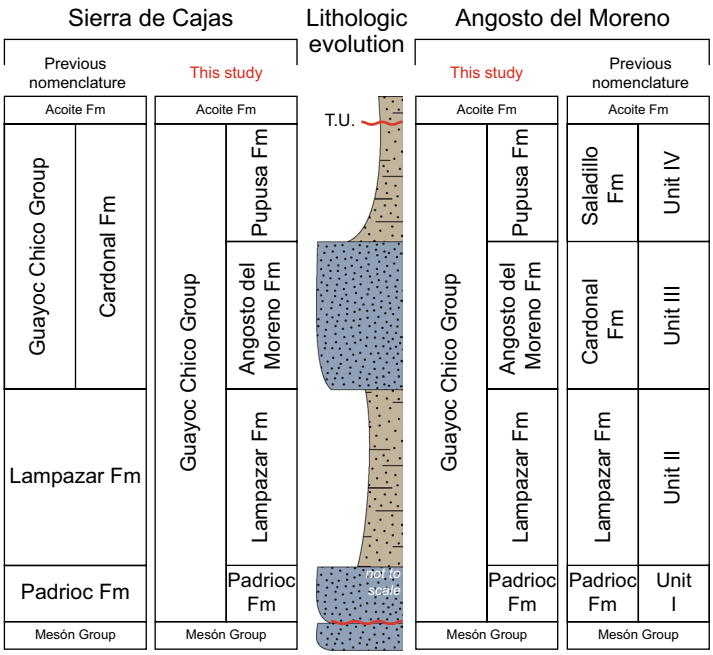

Fig. 3 Stratigraphic nomenclature update for the localities of Sierra de Cajas and Angosto del Moreno. The previously used nomenclature (see main text for details) is now updated providing easiest correlation between the western and the eastern part of Cordillera Oriental (Fig. 4). The Guayoc Chico Group is bracketed between the Mesón Group and the Tumbaya Unconformity, encompassing Pardioc, Lampazar, Angosto del Moreno and Pupusa formations. T.U., Tumbaya Uncomformity. Refer to Fig. 4, for the lithological pattern

sequence-stratigraphic and biostratigraphic study. In contrast, for the western border of the Cordillera Oriental and Salinas Grandes area (i.e., Sierra de Cajas and Angosto del Moreno; Figs. 2 and 3), formational names largely derive from uncertain correlations. Ramos (1973) proposed the Guayoc Chico Group to include the Lampazar, Cardonal, and Saladillo formations in this area (Fig. 3). These names were previously used by Harrington (1957), partially based on Keidel (in Harrington 1937), for the successions exposed in the Incamayo region (south of Angosto del Moreno; Fig. 2). However, subsequent authors (e.g., Malanca and Brandán 2000; Moya and Monteros 2000) did not use the names Santa Rosita Formation nor Guayoc Chico Group but referred these successions to Lampazar, Cardonal, and Saladillo formations (Fig. 3). Astini (2003, 2005) indicated that these formations should not be extended from Incamayo to Salinas Grandes due to substantial stratigraphic differences between these regions. Astini (2003, 2008), therefore, restricted the use of the Guayoc Chico Group for the Angosto del Moreno area, excluded from this group the Lampazar Formation, and proposed five informal members for the interval that Ramos (1973) and subsequent authors referred to as the Cardonal and Saladillo formations. Following the idea of not using previously defined formational names for the Angosto del Moreno area, Buatois et al. (2003) and Moya et al. (2003) proposed an informal stratigraphic framework that included four units (I, II, II, IV; Fig. 3).

Based on a biostratigraphically well-constrained, sedimentologic and stratigraphic study, it is here suggested to retain the Guayoc Chico Group for the succession bracketed between the Mesón Group and the Tumbaya Unconformity (Moya 1997) that separates this stratigraphic interval from the Acoite Formation (Fig. 3). Thus, the Guayoc Chico Group encompasses the Padrioc, Lampazar, Angosto del Moreno, and Pupusa formations (Fig. 3). The last two names are proposed herein to replace the informal members/units of previous authors and are formally defined in Appendix 1. The Lampazar and Angosto del Moreno formations correspond to the Furongian *Neoparabolina frequens argentina* biozone, whereas the Pupusa Formation encompasses the early Tremadocian *Jujuyaspis keideli* and *Kainella andina* biozones of the scheme proposed by Vaccari et al. (2010) (Fig. 4). The same stratigraphic pattern is recognized for the Furongian to lower Tremadocian deposits of Sierra de Cajas (Fig. 3).

Geologic and stratigraphic framework

The Cordillera Oriental represents one of the regions (with the Puna, the Sierras Subandinas, and the Sierra de Famatina; Figs. 1 and 2) exposing Cambrian-Ordovician strata in northwest Argentina. These strata were deposited along the proto-Pacific margin of Gondwana. Nowadays, the remains of this basin extend across northwest Argentina, north Chile, Bolivia and, Peru (Fig. 1; e.g., Astini 2003 and references therein). The oldest exposed rock in the Cordillera Oriental is the Ediacaran—Fortunian metasedimentary Puncoviscana Formation and equivalents (Figs. 2 and 4; e.g., Aceñolaza et al. 1988; Omarini et al. 1999; Augustsson et al. 2011; Escayola et al. 2011). This stratigraphic unit was subsequently exhumed during the early Cambrian Pampean Orogeny (e.g., Mon and Hongn 1996; Escayola et al. 2011; Casquet et al. 2018). Further, sandstone

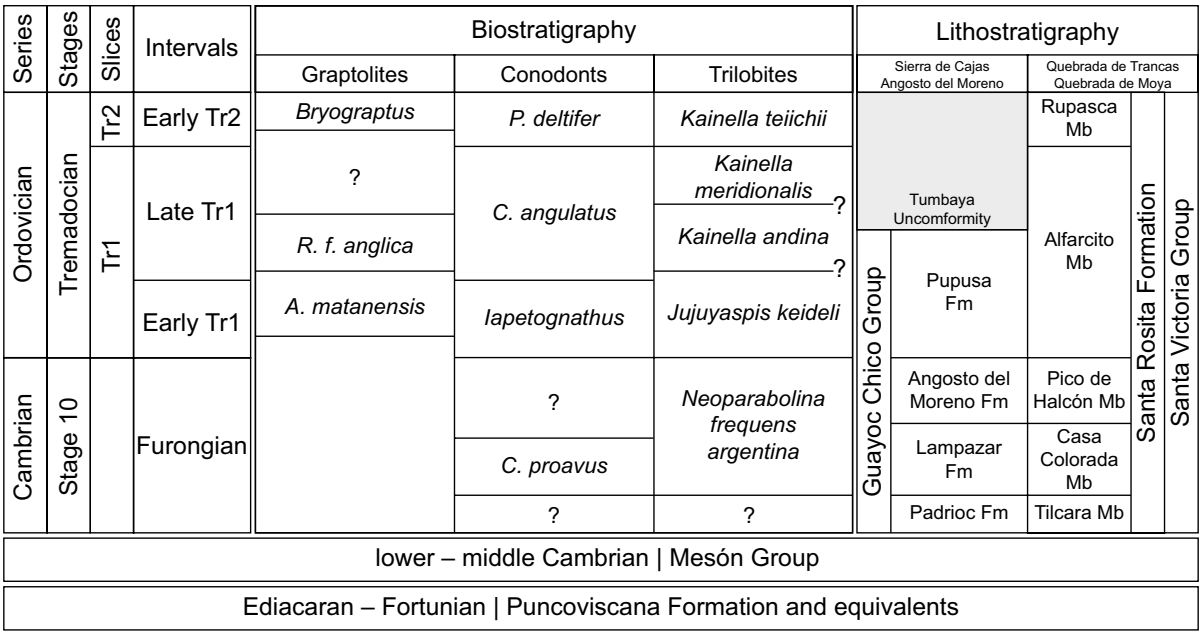

Fig. 4 Regional biostratigraphy and lithostratigraphy, correlated to the chart intervals used. Modified and updated form Balseiro and Waisfeld (2013). Note that the Humacha Member (the uppermost official member of the Santa Rosita Formation), which comes above the Rupasca Member is not shown since it is not part of this study

and mudstone of the lower to middle Cambrian Mesón Group unconformably overlie the Puncoviscana Formation and equivalents (Fig. 4; Sánchez and Salfity 1999; Mángano and Buatois 2004; Buatois and Mángano 2005; Augustsson et al. 2011). In the Cordillera Oriental, the upper Cambrian—Lower Ordovician Santa Victoria Group unconformably overlies the Mesón Group (Fig. 4; Moya 1988; Sánchez and Salfity 1999). On one hand, the contact between the Santa Victoria and the Mesón groups is considered as an unconformity related to extensive movements (Irúyica Event; Turner and Méndez 1975; Mon and Salfity 1995). Alternatively, this contact has been considered as an unconformity generated by a relative sea-level fall (e.g., Moya 1998; Buatois et al. 2000; Buatois and Mángano 2003; Mángano and Buatois 2004) or as a conformable depositional transition (e.g., Ruiz Huidobro 1975; Fernández et al. 1982). The Santa Rosita Formation and coeval strata may have been deposited after this opening phase, recording mostly long-term relative sea-level fluctuations (Moya 1988; Mon and Salfity 1995; Astini 2003; Buatois and Mángano 2003; Buatois et al. 2006).

The Santa Victoria Group encompasses the Santa Rosita Formation (upper Cambrian; Stage 10—Lower Ordovician; Tr1—Tr3) and the Acoite Formation (Lower Ordovician; Floian—Dapingian) (Turner 1960; Toro and Herrera Sánchez 2019). The Santa Rosita Formation is divided into six members, namely Tilcara, Casa Colorada, Pico de Halcón, Alfarcito, Ruspaca, and Humacha members, in stratigraphic order (Fig. 4). The Guayoc Chico Group is coeval with the lower part of the Santa Rosita Formation that is divided into four formations, namely Padrioc, Lampazar, Angosto del Moreno and Pupusa (Figs. 3 and 4). In all places, the Tilcara Member and the Padrioc Formation overlain the Mesón Group (e.g., Turner 1960; Moya 1988). In Sierra de Cajas and Angosto del Moreno, the sedimentary successions belong to the Guayoc Chico Group, whereas in Quebrada de Trancas and Quebrada de Moya, the stratigraphic successions are part of the Santa Rosita Formation (Figs. 3 and 4).

Methodology

Sedimentology and Stratigraphy

Sedimentologic field-based studies were undertaken in Cambrian-Ordovician sedimentary rocks of the Cordillera Oriental (Figs. 1 and 2) in northwest Argentina. The first step involved logging at a decimeter-scale of approximately 1700 m of cumulative thickness from four different sedimentary successions (namely Sierra de Cajas, Angosto del Moreno, Quebrada de Trancas, and Quebrada de Moya; see Figs. 1, 2 and 5). Lithology, grain size, sedimentary structures, beds thickness, bed contacts, and overall geometries were described, allowing the distinction of sedimentary facies that were grouped into four facies assemblages. Due to the extent of the studied area (~ 1500 km^2) and the thickness of the deposits, the classic continental to shallow-marine subdivisions (e.g., Walker and James 1992; Clifton 2006; Plint 2010) have been simplified to

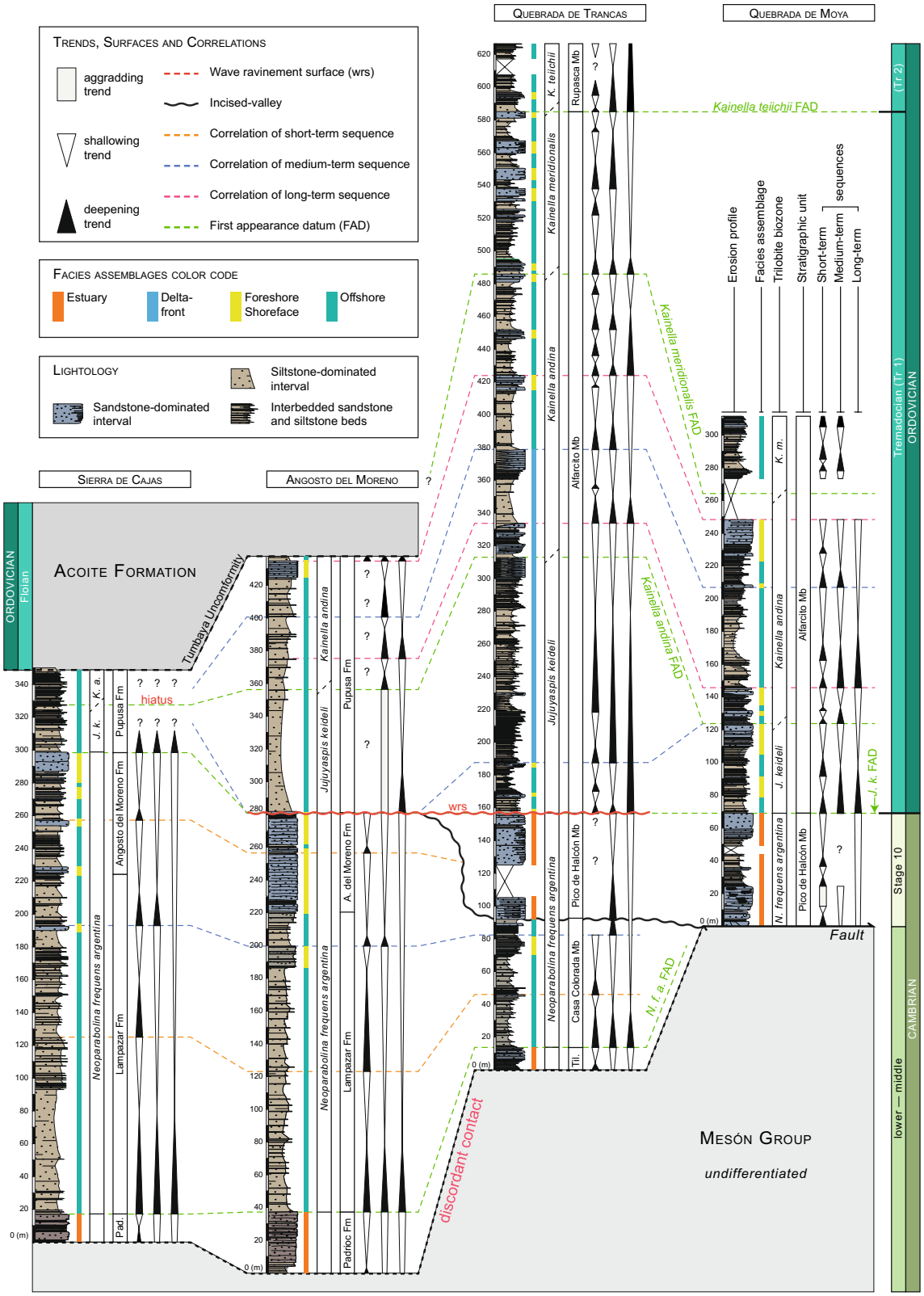

Fig. 5 Detailed stratigraphic sections encompassing the Cambrian-Ordovician boundary. Sequence stratigraphic and biostratigraphic correlations among localities are shown. *Pad.,* Padrioc Formation; *N.f.a.*, *Neoparabolina frequens argentina; J.k.*, *Jujuyaspis keideli*; *K.*, *Kainella*; *K.m., Kainella meridionalis*

allow for reconstruction of basin evolution. Accordingly, fluvial and tidal-influenced marginal-marine systems are here grouped as Estuary facies assemblages; foreshore, upper, middle and lower shoreface deposits composed the Foreshore-Shoreface facies assemblages (i.e., between mean sea-level and the fair-weather wave base; FWWB); distal and proximal delta-front facies constitute the Delta-front; and offshore transition, upper and lower offshore deposits are referred to as the Offshore facies assemblages (i.e., from the fair-weather wave base to the storm wave base). An integrative approach describing the basin evolution is then proposed for the Cordillera Oriental across the Cambrian-Ordovician transition. Further, this study is placed in a broader context incorporating adjacent basins.

Biostratigraphy

Trilobites provide temporal control as this is the most accurate fossil group for the studied interval (Fig. 4). The earliest trilobite-bearing strata correspond to the base of the Lampazar Formation and the Casa Colorada Member (Figs. 4 and 5) recording the first appearance datum (FAD) of *Neoparabolina frequens argentina* (Vaccari et al. 2010). One isolated remain of *Neoparabolina frequens argentina* has been found in the uppermost strata of the Padrioc Formation at Angosto del Moreno (Moya and Monteros 2000). The Cambrian-Ordovician boundary is identified in our studied area by the FAD of *Jujuyaspis keideli* (Figs. 4 and 5). According to Vaccari et al. (2010, 2018), the classic fossil distribution through the *Jujuyaspis keideli* biozone starts with the FAD of *Jujuyaspis keideli* followed by the FAD of *Saltaspis steinmanni*. At Angosto del Moreno, only *Saltaspis steinmanni* was found, therefore lacking the lower interval of the *J. keideli* biozone. The early Tremadocian (Tr1; Early Ordovician) consists of the *Jujuyaspis keideli, Kainella andina,* and *Kainella meridionalis* biozones (e.g., Vaccari et al. 2010 and references therein). The upper limit of the *Kainella meridionalis* biozone corresponds to the Tr1—Tr2 boundary, and is marked by the FAD of *Kaninella teiichii.*

Results

The Santa Rosita Formation and the Guayoc Chico Group chiefly consist of muddy siltstone interbedded with medium- to very fine-grained sandstone. Thirteen sedimentary facies gathered into the four facies assemblages previously listed (i.e., Estuary, Foreshore-Shoreface, Delta-front, and Offshore; Table 1), were identified.

Estuary

Description

This facies assemblage consists of three sedimentary facies (E1, E2, E3; Table 1; Fig. 6). E1 is composed of unbioturbated fine- to medium-grained sandstone units (individual beds > 1 m thick) with irregular bases. Sandstone commonly displays trough-cross bedding and some bed surfaces shown mudstone intraclasts (Fig. 6a). This facies occurs in the Tilcara Member in Quebrada de Trancas. E2 consists of trough cross-bedded fine- to medium-grained sandstone (Fig. 6c). Single and double mudstone drapes occur on the foreset of the cross-stratified sandstone (Fig. 6c). Units may reach up to several meters thick, are poorly bioturbated, and have an overall lenticular geometry (Fig. 6b). The axes of E2 sandbodies are oriented south/north (Fig. 6b). E3 comprises heterolithic packages exhibiting wavy-, flaser- and lenticular-bedded sandstone layers alternating with muddy-siltstone. E3 is also poorly bioturbated. In some localities, ladderback ripples (Fig. 6d) on bed tops were observed, as well as syneresis cracks. Both E2 and E3 are present in the Pico de Halcón Member in Quebrada de Trancas and Quebrada de Moya, as well as in the Padrioc Formation in Sierra de Cajas and in Angosto del Moreno.

Interpretation

Trough cross-stratification indicates a unidirectional tractional flow and migration of 3D dunes. The associated mudstone intraclasts suggest the interplay of fluvial and tidal processes along the fluvial to the marine transition zone, where high-energy currents (tidal and fluvial) were capable of reworking previously deposited mudstone layers (e.g., Gugliotta et al. 2018). The absence of bioturbation suggests strongly brackish to freshwater conditions, preventing colonization by the infauna (Mángano and Buatois 2003). Together, these observations suggest deposition in fluvial-tidal channels. Paleocurrent data from 3D dunes show a northward progradation. Sandstone beds displaying trough cross-bedding (E2) and mudstone drapes point to subaqueous dunes that migrated northward in tidal channels (Dalrymple and Choi 2007). Heterolithic facies (E3) intervals reflect deposition in tidal flats (Buatois and Mángano, 2003; Buatois et al. 2006), and resemble similar deposits elsewhere (e.g., Collinson et al. 2006; Dalrymple and Choi 2007). The association of the three sedimentary facies points to estuarine environments (Buatois and Mángano 2003; Buatois et al. 2006).

Table 1 Sedimentary facies characteristics and facies assemblages

Facies Assemblage	Facies	Dominant lithology	Dominant sedimentary structures	Bed thickness	Associated lithology and sedimentary structures	Bed contacts and organization	Environment
Estuary	*E1*	Fine- to medium-grained sandstone	Trough cross-stratification	> 1 m	Mudstone clasts	Erosive base, overall lenticular	Fluvial-tidal channel
	E2	Medium-grained sandstone	Tangential cross-stratification	~ 50 cm	Mostly unidirectional, bidirectional, simple to double mudstone drapes	Erosive base, overall lenticular	Tidal channel
	E3	Heterolithic	Wave and current ripples	~ 10 cm	Ladderback ripples at the top of the sandstone beds alternating with siltstone beds; wavy-, flaser-, lenticular-beddings; synaeresis cracks	Sharp base, rhythmic alternation of sandstone and siltstone layer	Tidal flat
Foreshore- Shoreface	*FS1*	Fine- to medium-grained sandstone	Low angle parallel stratification (swash cross-stratification)	~ 80 cm	keystones vugs	Erosive base, tabular, undulate	Foreshore (tide-modulated)
	FS2	Fine- to medium-grained sandstone	Wave and current ripples	~ 10 cm	–	Erosive base, tabular, undulate	Foreshore (tide-modulated)
	FS3	Very fine- to medium-grained sandstone	Trough cross-stratification and hummocky cross-stratification	~ 30 cm	Wave ripple, combined flow ripples	Erosive base, tabular	Upper to lower shoreface
	FS4	Poorly sorted matrix-supported breccia	–	~ 80 cm	Sandstone matrix, centimeteric to decimeteric pebble-to cobble-sized sandstone to siltstone clasts	Erosive base, tabular	Transgressive shoreface
Delta-front	*DF1*	Fine- to medium-grained sandstone	Planar bedding with local bed pinch-out, planar lamination, current ripples	~ 80 cm	Amalgamated packages, soft-sediment deformation, current ripples	Erosive base, lobate-shaped, laterally discontinuous	Proximal delta-front
	DF2	Siltstone with subordinate sandstone layer	–	~ 2 cm	Thin intercalations of fine-grained sandstone layer with combined-flow ripples	Erosive base, tabular	Distal delta-front
Offshore	*O1*	Mudstone, muddy siltstone to siltstone	–	~ 1 cm	Thin intercalations of very fine-grained sandstone with parallel stratification, combined-flow and wave ripples	Sharp, locally erosive base, tabular	Lower offshore
	O2	Grainstone	Wave ripples	~ 5 cm	–	Sharp base, tabular	Lower offshore
	O3	Very fine-grained sandstone and siltstone	Scour-and-drape hummocky cross-stratification and microhummocky cross-stratification (decimetre-scale wavelength)	~ 10 cm	Interference ripples at the top, gutter casts, flute casts	Erosive base, tabular	Upper offshore

Table 1 (continued)

Facies Assemblage	Facies	Dominant lithology	Dominant sedimentary structures	Bed thickness	Associated lithology and sedimentary structures	Bed contacts and organization	Environment
	O4	Very fine- to fine-grained sandstone	Scour-and-drape hummocky cross-stratification (metre-scale wavelength)	~30 cm	Interbedded siltstone, bioclastic layers may occur interference ripples at the top, soft-sediment deformation structures at the base, gutter casts, flute casts	Erosive base, tabular	Offshore transition

Foreshore-Shoreface (FS)

Description

This facies assemblage consists of four sedimentary facies (FS1, FS2, FS3, FS4; Table 1, Fig. 7). FS1 comprises low-angle planar-laminated unbioturbated fine- to medium-grained sandstone (i.e., swash cross-stratification) with aligned pores with a millimeter-scale diameter (Fig. 7a). FS2 are sandstone having symmetrical to asymmetrical ripples and rare trace fossils (Fig. 7a). FS1 and FS2 occur only at Sierra de Cajas at the top of the Angosto del Moreno Formation. These beds exhibit normal contacts but have lateral thickness variations, reaching up to *ca*. 12 m thick. FS3 comprises up to 1-m thick, hummocky cross-stratified to trough cross-stratified very fine- to fine-grained sandstone (Fig. 7b) with symmetrical (Fig. 7c) to asymmetrical ripples (Fig. 7d), occurring in all localities in the Lampazar and Angosto del Moreno formations, and in the Alfarcito and Rupasca members (Fig. 5). Individual beds are stacked forming up to 10 m thick stratigraphic packages and bioturbation is scarce typically represented by *Skolithos linearis*. This facies is present in all localities. FS4 corresponds to unbioturbated erosionally based, poorly-sorted, matrix-supported breccia forming beds up to 80 cm thick (Fig. 7e). FS4 was only identified at Quebrada de Trancas at the base of the Alfarcito Member (Fig. 7e). Breccia is characterized by a sandy matrix with pebble-to cobble-sized sandstone to siltstone clasts (Fig. 7e).

Interpretation

Planar bedding in FS1 likely reflects high-energy, upper-flow regime processes (e.g., Perillo et al. 2014). The associated aligned pores are considered as keystone vugs formed by air-bubble trapped in the sediment by swash processes (e.g., Dunham 1970; Reineck and Singh 1980). Symmetrical and asymmetrical ripples in FS2 reflect oscillatory to combined-flow processes, which are likely formed by the interplay of wave and tide processes. The stacking pattern of FS1 and FS2 reflects deposition in a wave-dominated, tidally modulated foreshore, where surf-swash processes (at low tide; FS1) alternated periodically with oscillatory processes (at high tide; FS2) (e.g., Vaucher et al. 2017, 2018). FS3 exhibits sedimentologic features pointing to deposition from permanent, nearshore oscillatory, unidirectional and combined-flow currents acting at the water–sediment interface and punctuated by storm events in shoreface environments as discussed in previous studies in these strata (Buatois and Mángano 2003; Buatois et al. 2006) and elsewhere (e.g., Hampson and Storms 2003; Clifton 2006). The presence of vertical burrows of suspension feeders (i.e., *Skolithos linearis*) indicates high-energy conditions and organic particles in suspension in the water column, consistent with

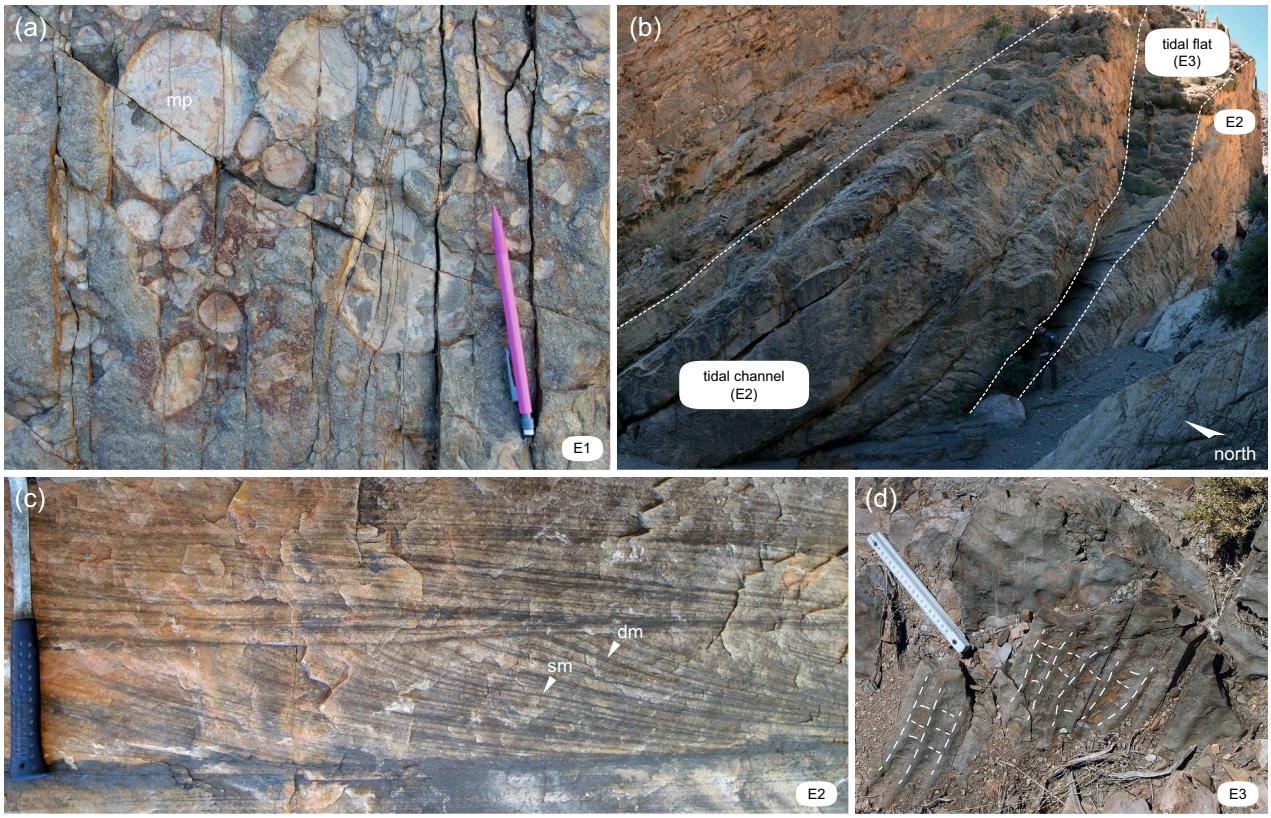

Fig. 6 Estuary facies zone. **a** Mudstone pebble on the top of the surface of a sandstone bed (E1); Tilcara Member; Quebrada de Trancas. *mp*: mudstone pebble. **b** Sandstone beds reflecting the infill of tidal channels (E2); Pico de Halcón Member; Quebrada de Moya. Person for scale is 1.75 m. **c** Trough cross-stratified sandstone and associated mudstone drapes (E2); Pico de Halcón Member; Quebrada de Trancas. *sm,* single mudstone drap; *dm,* double mudstone drapes. **d** Ladder-back ripples (E3); Padrioc Formation; Sierra de Cajas. Dashed line highlights the crests of ladder-back ripples

deposition in agitated nearshore areas (Mángano et al. 2005). Breccia beds of FS4 reflect high-energy deposition and pass vertically to offshore deposits (see "Offshore (O)"). FS4 potentially records wave-ravinement processes during a transgressive phase (e.g., Cattaneo and Steel 2003; Buatois et al. 2012; Zecchin et al. 2018).

Delta-Front (DF)

Description

This facies assemblage contains two sedimentary facies (DF1, DF2; Table 1; Fig. 8). DF1 consists of fine-grained sandstone forming packages of *ca.* 2–10 m thick (Fig. 8a– c, e, f). DF1 is characterized by planar bedding with local bed pinch-out, planar lamination, and asymmetrical ripples. Soft-sediment deformation structures are found near the sandstone bases (Fig. 8c). DF1 is laterally discontinuous and shows an overall lobate geometry (Fig. 8a, e, f). This facies pinches out westwards and eastwards into DF2 siltstone intervals at the scale of hundreds of meters (Fig. 8a, e). DF2 is composed of thick, continuous, homogeneous siltstone intervals (Fig. 8a), locally intercalated with cross-laminated very fine-grained sandstone (Fig. 8d). Body and trace fossils are scarce and poorly diverse in DF1 and DF2. Both facies are only present in the Alfarcito Member at Quebrada de Trancas (Fig. 5).

Interpretation

Lobe morphologies suggest the dominance of unidirectional flows likely driven by river processes combined with a high rate of sedimentation without substantial reworking of material by strong waves (e.g., Reading and Collinson 1996; Bhattacharya and Giosan 2003; Bhattacharya et al. 2006). Only a few oscillatory structures were observed, suggesting limited wave/storm influence. The sandstone units likely reflect deposition in more proximal settings, whereas

Fig. 7 Foreshore-shoreface facies zone. **a** Sandstone bed displaying low-angle planar stratification (in orange; FS1) alternated with thinner sandstone levels exhibiting small-scale symmetrical and asymmetrical ripples (in yellow; FS2); Sierra de Cajas, Angosto del Moreno Formation. Note that rippled intervals have a very limited lateral extension. **b** Trough cross-stratified sandstone (FS3) with superimposed wave ripples (wr); Alfarcito Member; Quebrada de Moya. **c** Sandstone (FS3) with aggrading symmetrical ripples suggesting high sedimentation rate; Sierra de Cajas, Angosto del Moreno Formation. **d** Sandstone (FS3) with wave and combined-flow cross-lamination; Quebrada de Trancas; Alfarcito Member. **e** Poorly sorted, matrix-supported breccia (FS4) corresponding to the basal levels of Alfarcito Member at Quebrada de Trancas

siltstone intervals suggest more distal emplacement. Lateral pinchouts between the two facies are evidence of northward progradation. The lobate shape of sandstone bodies suggests that adjacent siltstone intervals record deposition away from major terrestrial inputs. Furthermore, the combined reduced fossil content and the scarce bioturbation could reflect stressed environments related to freshwater input and high sediment concentration in the water column (e.g., MacEachern et al. 2005). This facies assemblage points to a river-dominated, wave-affected proximal (DF1) to distal (DF2) delta front (e.g., Orton and Reading 1993; Olariu and Bhattacharya 2006; Coates and MacEachern 2007).

Offshore (O)

Description

This facies assemblage is composed of four sedimentary facies (O1, O2, O3, O4; Table 1; Fig. 9). O1 consists of laterally persistent poorly bioturbated to unbioturbated, sharp-based, meter-thick mudstone and siltstone packages (Fig. 9a), interbedded with centimetre-thick, very fine-grained sandstone layers displaying parallel stratification, combined-flow cross-lamination, as well as symmetrical ripples. O2 comprises unbioturbated bioclastic grainstone (sensu Lokier and Al Junaibi 2016). It consists of decimetre-thick fossil-rich (mostly trilobite and echinoderm remains), wavy sandy limestone layers that can form up to 2 m-thick packages. O3 consists of siltstone packages interbedded with discrete hummocky to microhummocky cross-stratified, very fine-grained sandstone, in places displaying interference ripples (Fig. 9b–d). O4 comprises regularly interbedded discrete hummocky cross-stratified very fine- to fine-grained sandstone and thin siltstone intercalations (Fig. 9e). Both O3 and O4 include sandstone layers with sharp bases contact showing flute and gutter casts and flame structures. Gutter casts are all oriented north–south (Fig. 9d), and flute casts indicate a northward direction of the paleoflow (Fig. 9f). With the exception of O2, only found at the base of the Lampazar Formation in Sierra de Cajas, all the sedimentary facies that composed this facies assemblage are the most commonly found at the different localities and are present in the Lampazar and the Pupusa formations, and in the Casa Colorada, the Alfarcito and the Rupasca members (Fig. 5). Overall, this facies assemblage contains abundant and diverse trace fossils. Body fossils are mainly represented by trilobites and brachiopods.

Interpretation

This facies assemblage records deposition below the FWWB in open marine offshore environments, reflecting low-energy suspension fall-out conditions punctuated by storm events at various depths (e.g., Heward 1981; Buatois et al. 2006; Clifton 2006; Vaucher et al. 2017). According to the previously described facies zone (i.e., Delta-front), a prodeltaic setting for some siltstone intervals displaying very thin fine-grained sandstone layer cannot be excluded (e.g., Coates and MacEachern 2007; Bhattacharya and MacEachern 2009). The sandy limestone intervals exclusively composed of shelly remains (mostly trilobite) seem to reflect low sedimentation rates during a transgressive phase (e.g., Beckvar and Kidwell 1988; Botquelen et al. 2004). Ichnologic information supports deposition in fully marine, distal settings (Mángano et al. 2005), which is consistent with body-fossil data.

The Cambrian-Ordovician unconformity

In Quebrada de Trancas, the lowermost Ordovician strata consist of shallow-marine deposits (base of Alfarcito Member; Figs. 5, 10a and b) that truncate the underlying estuarine Cambrian deposits (Pico de Halcón Member), suggesting that up to 25 m of strata are missing. The erosion surface is overlain by breccias of FS4 (Fig. 7e) that grade upward into offshore deposits (Fig. 5). At this locality, Lower Ordovician deposits onlap the underlying Cambrian strata (Fig. 10a). Measured dips of the beds above and below the erosion surfaces are 60° and 50°, respectively, suggesting an angular unconformity. On the southern flank of the Angosto del Moreno (Fig. 10c), three upper Cambrian sandstone units (foreshore-shoreface deposits of the Angosto del Moreno Formation) are juxtaposed against the Lower Ordovician siltstone unit (offshore deposits of the Pupusa Formation). In the northern part (Fig. 10c), the upper Cambrian foreshore-shoreface deposits (Angosto del Moreno Formation) are sharply overlain by Lower Ordovician offshore deposits (Pupusa Formation), suggesting that up to 60 m of strata were removed along the surface. Contrarily to Quebrada de Trancas, no breccia was found at the contact between Cambrian and Ordovician rocks.

The erosive and unconformable stratigraphic surface, separating the marginal-marine units below (i.e., Pico de Halcón Member at Quebrada de Trancas / Angosto del Moreno Formation at Angosto del Moreno) from the overlying deeper-water, fully marine deposits (i.e., Alfarcito Member at Quebrada de Trancas/Pupusa Formation at Angosto del Moreno), is interpreted as a wave ravinement surface (Cattaneo and Steel 2003; Zecchin et al. 2018 and references therein). In a high-energy context, erosion by wave ravinement is commonly able to remove up to 10–20 m of sediment (e.g., Cattaneo and Steel 2003; Zecchin et al. 2018). However, ~ 25 m and ~ 60 m have been removed in Quebrada de Trancas and Angosto del Moreno, respectively (Fig. 10a, c). This suggests a slow landward retreat of the shoreline, allowing longer time for waves to remove the underlying sediment (Zecchin et al. 2018). The angular relationship observed in Quebrada de Trancas suggests that the wave ravinement surface was formed on a steep profile, implying uplift that tilted the Pico de Halcón Member prior to deposition of the Alfarcito Member. Deposits associated with wave ravinement are commonly millimeter to decameter thick. However, the unusual thickness (~ 80 cm) of the breccia beds found at Quebrada de Trancas suggests a high-gradient topography (e.g., Hwang and Heller 2002; Zecchin et al. 2018), also supporting a cliff-like configuration of tilted Cambrian sedimentary strata prior to the formation of the wave ravinement surface. In the two other studied localities, Sierra de Cajas and Quebrada de Moya, the absence of outcrop continuity

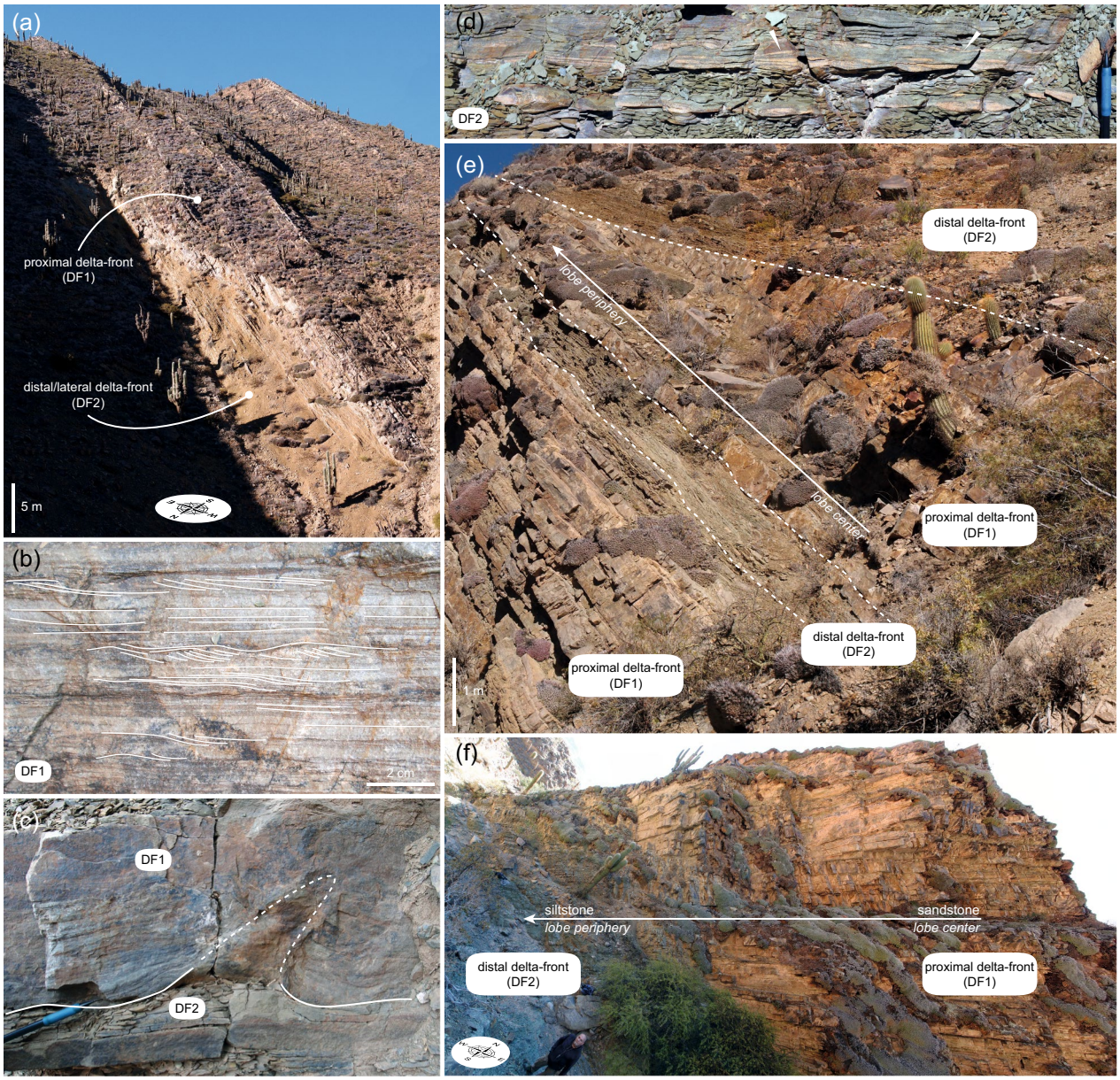

Fig. 8 Delta-front facies zone in Quebrada de Trancas; Alfarcito Member. **a** Lobe sandstone complex (DF1) with the axis toward the north laterally pinching out into a siltstone interval (DF2). **b** Fine-grained sandstone (DF1) displaying current-ripples and planar-laminations. **c** Soft-sediment deformation structures near the bottom of a sandstone bed. **d** Siltstone interval (DF2) with intercalated cross-laminated fine-grained sandstone (pointed out by the white arrows). **e** Stacking pattern highlighting the vertical relationship between proximal (DF1) and distal (DF2) delta-front and the lobate geometry of DF1. **f** Central view of a lobate sandstone package (DF1) showing the lateral relationship with the adjacent siltstone interval (DF2)

prevent closer examination of the stratal geometries associated with the Cambrian-Ordovician boundary.

Depositional model

Late Cambrian (Furongian)

The oldest depositional units of the studied interval correspond to the Tilcara Member and the Padrioc Formation (late Cambrian; Furongian; Figs. 4 and 5), which overlie the Mesón Group. Both units reflect proximal estuarine environments characterized by fluvial-tidal channels (Figs. 5 and 6a;

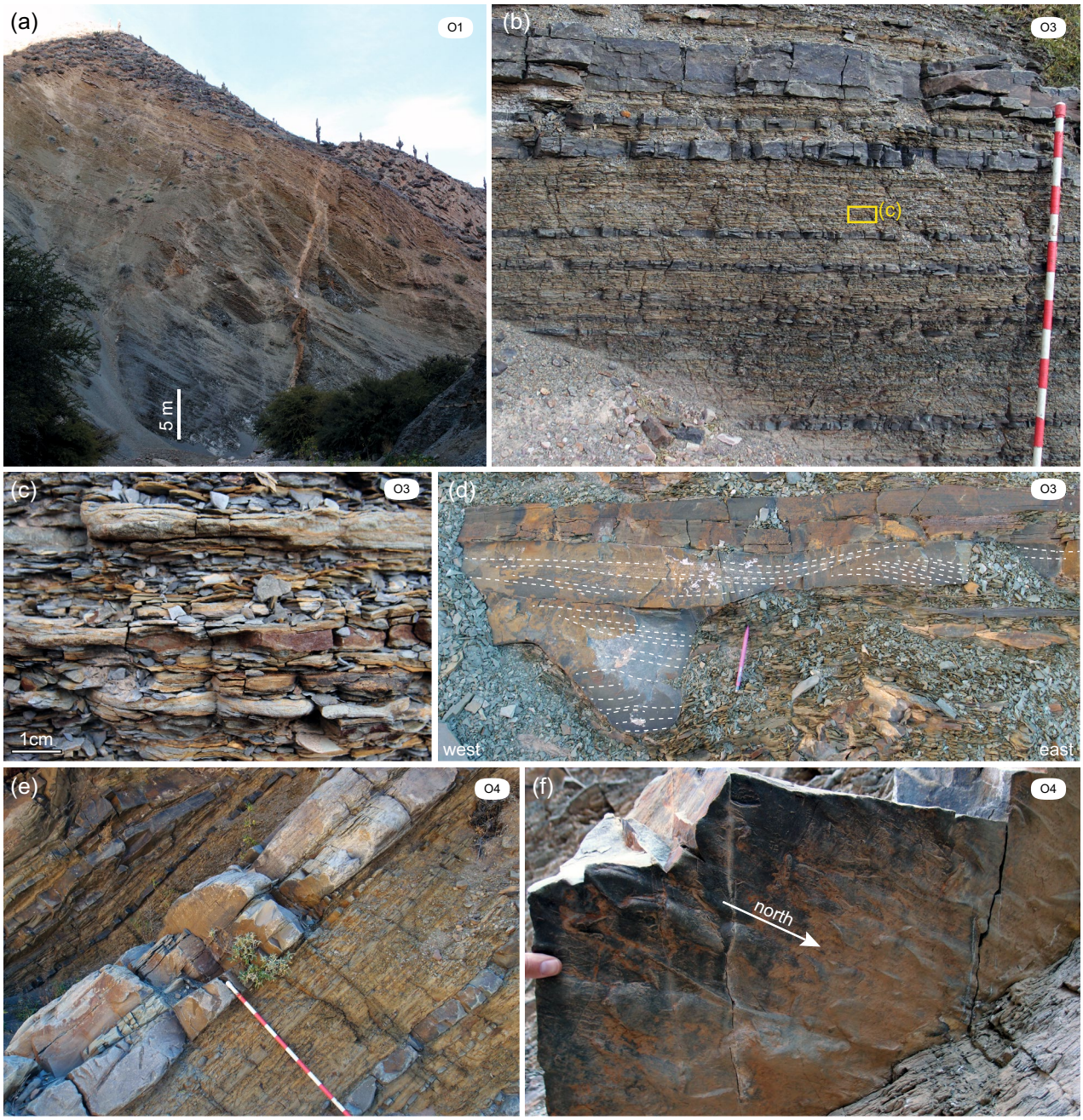

Fig. 9 Offshore facies zone. **a** Overview of the siltstone-dominated intervals (O1); Quebrada de Moya; Alfarcito Member. **b** Siltstone interbedded with hummocky cross-stratified sandstone; Quebrada de Moya; Alfarcito Member (O3). **c** Close-up of **b** showing intercalated sandstone and siltstone layers at centimeter-scale. **d** Hummocky cross-stratified sandstone displaying a steep-sided gutter cast, Quebrada de Trancas, Alfarcito Member (O3). **e** Hummocky cross-stratified sandstone intercalated within sandy siltstone (O4), Quebrada de Trancas, Alfarcito Member. **e** North-directed flute casts at the base of a sandstone bed (O4), Quebrada de Moya; Alfarcito Member

Table 1), corresponding to a lowstand systems tract (LST) and an early transgressive systems tract (TST; Buatois et al. 2006), open to the north, as suggested by paleocurrent data showing a south-to-north tidal transport.

The TST is recorded by offshore environments identified by a siltstone-dominated interval interbedded with storm-induced deposits (O1; O3; O4; Figs. 5 and 9). This TST corresponds to the Lampazar Formation and the coeval Casa Colorada Member (Figs. 4 and 5). The base of these units is mostly coincident with the FAD of *Neoparabolina frequens argentina* (Figs. 4 and 5). A long-term retrogradational trend characterized the Cambrian interval but is punctuated by a first regressive pulse that mostly delineates the tops of both the Lampazar Formation (at 192 m in Sierra de Cajas; at

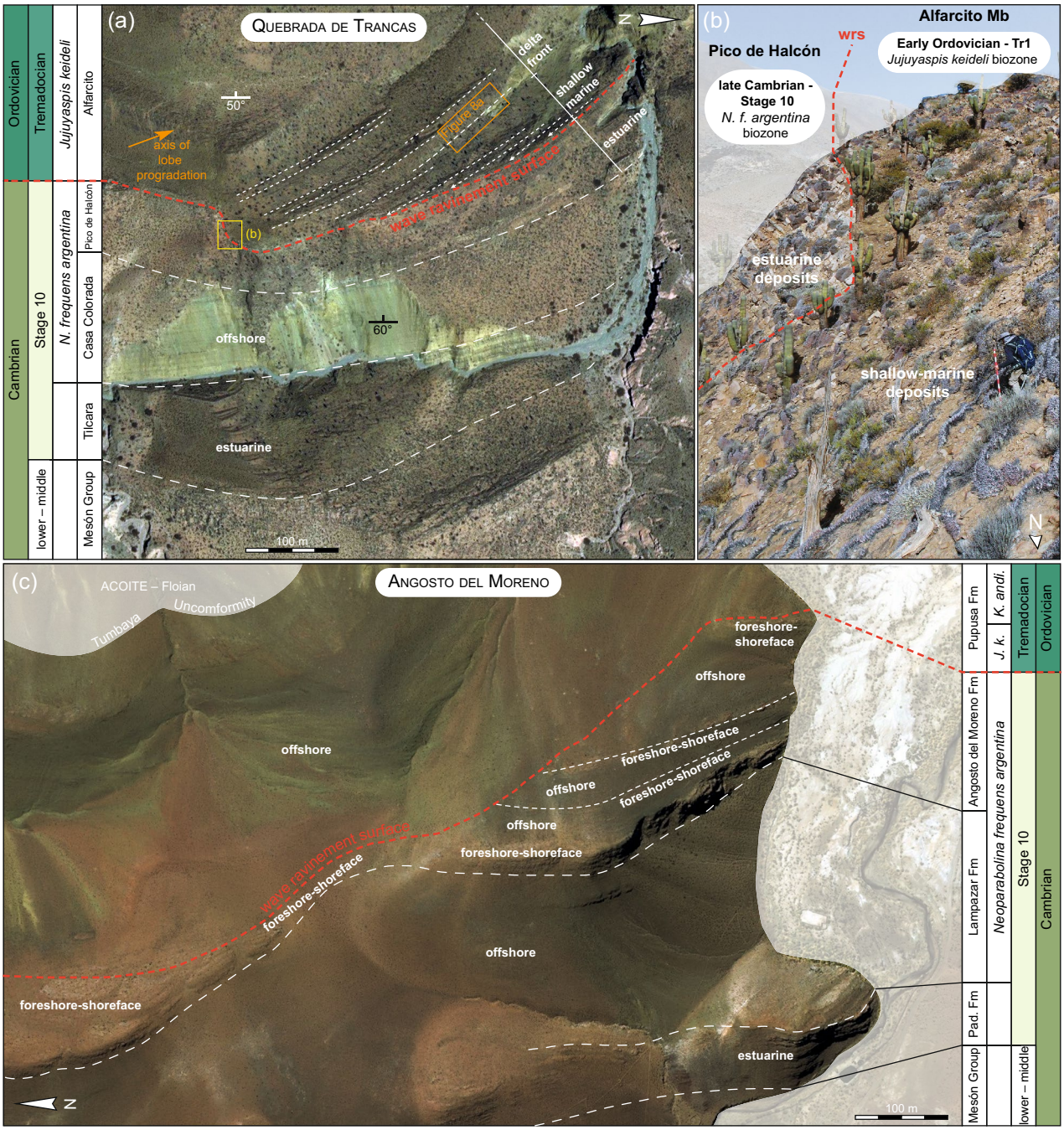

Fig. 10 Cambrian-Ordovician unconformity. **a** Satellite view from Quebrada de Trancas highlighting the discordant and erosional contact between the upper Cambrian Pico de Halcón Member with the overlying lower Tremadocian Alfarcito Member. **b** Field observation of the wave ravinement surface (wrs) between Pico de Halcón and Alfarcito members. Person for scale is 1.7 m. **c** Satellite view from Angosto del Moreno showing the wave ravinement surface. The northern part shows a conformable contact between upper Cambrian and Lower Ordovician strata, while in the southern flank three upper Cambrian units are juxtaposed to Lower Ordovician siltstone. Satellite images are from Bing Maps ©

200 m in Angosto del Moreno; Fig. 5) and the Casa Colorada Member (at 82 m in Quebrada de Trancas; Fig. 5). The Casa Colorada Member is not present in Quebrada de Moya, because the Pico de Halcón Member has a faulted contact with the underlying Mesón Group.

By the end of the Cambrian, a major regressive phase took place as reflected by the deposition of the highstand systems tract (HST) sandstone-dominated Angosto del Moreno Formation at both Sierra de Cajas and Angosto del Moreno. This HST phase is characterized by the

emplacement of foreshore-shoreface environments (Figs. 5 and 7). In Quebrada de Trancas and Quebrada de Moya, the estuarine Pico de Halcón Member represents the subsequent LST and TST displaying a northward orientation of the system as exhibited by axes of incision of the estuarine channels (Figs. 5 and 6). The estuarine Pico de Halcón Member fills an incised valley (Buatois et al. 2006). This implies that the underlying deposits (i.e., Angosto del Moreno Formation) were eroded in Quebrada de Trancas and Quebrada de Moya. In Sierra de Cajas, sharp-based shoreface to foreshore parasequence sets are observed (Fig. 5). At this locality, the Angosto del Moreno Formation commonly displays mostly offshore to lower shoreface deposits that are abruptly overlain by foreshore sandstones (Fig. 5). Such a stratigraphic pattern suggests a forced regression, which corresponds to a falling stage systems tract (FSST) (e.g., Clifton 2006). In the Angosto del Moreno, the Angosto del Moreno Formation almost exclusively displays shoreface deposits (Fig. 5), suggesting slightly deeper-water settings of deposition in comparison with Sierra de Cajas. The Angosto del Moreno Formation and the Pico de Halcón Member are the upper stratigraphic units belonging to the *Neoparabolina frequens argentina* biozone (Figs. 4 and 5), thus marking the end of Cambrian record.

Early Ordovician (Tr1)

The beginning of the Ordovician was characterized by a major transgressive phase during which the TST of the Pupusa Formation and the Alfarcito Member were deposited; both correspond to the base of *Jujuyaspis keideli* biozone (Figs. 4 and 5). The facies assemblage in the lower part of Tr1 (between 157 and 188 m; Fig. 5) indicates that wave-dominated conditions prevailed (foreshore-shoreface to offshore environments; Quebradas de Trancas and Moya; Figs. 5 and 11a), while coeval strata suggest offshore environments (Sierra de Cajas and Angosto del Moreno; Figs. 5 and 11a). A rapid change from wave-dominated conditions (lower shoreface—offshore deposits; TST) to river-dominated (distal to proximal delta-front environments; HST; at 188 m Fig. 5) is revealed by the presence of the siltstone-to-sandstone lobate interval (DF1 and DF2) of the delta-front facies assemblage (Figs. 5 and 7) in Quebrada de Trancas. This change is apparent several meters above the base of the *Jujuyaspis keideli* biozone, continuing up to the middle of the *Kainella andina* biozone (Fig. 5). In order to preserve the delta-front lobate sandstone (Fig. 8e, f) of the Alfarcito Member between 188 to 380 m (in Quebrada de Trancas; Fig. 5), reduced incoming wave energy is suggested (e.g., Reading and Collinson 1996; Bhattacharya and Giosan 2003; Bhattacharya et al. 2006).

The lower Tremadocian interval in Sierra de Cajas consists of two biozones (*Jujuyaspis keideli* and *Kainella andina*) identified in the much thinner Pupusa Formation (25 m thick in Sierra de Cajas and 165 m thick in Quebrada de Trancas; Fig. 5). Even though the Pupusa Formation is thinner in Sierra de Cajas compared to Angosto del Moreno, both *Jujuyaspis keideli* and *Saltaspis steinmanni* occur, which is not the case southward at Angosto del Moreno where only *Saltaspis steinmanni* was found. Therefore, the absence of *Jujuyaspis keideli* at Angosto del Moreno suggests that the TST at the base of the Pupusa Formation is diachronic with a north to south transgressive trend. Hence, to explain the reduced thickness of the Pupusa Formation in Sierra de Cajas and the absence of *Jujuyaspis keildeli*, an uplift at Angosto del Moreno and further in Sierra de Cajas is proposed. The uplift should have occurred prior to the deposition of the Pupusa Formation at Angosto del Moreno, thus exposing the Angosto del Moreno Formation during the Cambrian-Ordovician transition (Fig. 10c). Afterward, uplift took place in Sierra de Cajas, whereas the transgression continued, forming an extensive wave ravinement surface and leading to deposition of the transgressive Pupusa Formation at Angosto del Moreno (Fig. 10c). The uplift at Sierra de Cajas may have formed a high relief acting as a hydrodynamic barrier dissipating the incoming wave energy (Beji and Battjes 1993). This barrier allowed the preservation of lobate-shaped deposits (DF1 and DF2) in a protected southern area (Fig. 11b). During the uplift in Sierra de Cajas, the establishment of strong currents is proposed. These currents may have prevented sedimentation and/or removed sediments, therefore explaining the reduced thickness of the Pupusa Formation. In Sierra de Cajas, the contact between the *Jujuyaspis keideli* and *Kainella andina* biozones represents a sedimentary hiatus (Figs. 5 and 11b). Foreshore-shoreface sedimentation prevailed in Quebrada de Moya during the emplacement of the lobe deltaic (DF1) complex in Quebrada de Trancas. Quebrada de Moya is located slightly to the northeast of Quebrada de Trancas, but was under the influence of more energetic processes (i.e., fair-weather and storm waves). Therefore, Quebrada de Moya contributed to produce a protected environment in Quebrada de Trancas. Such conditions very likely happened during the deposition of the deltaic lobes (i.e. up to the middle of *Kainella andina* biozone; at 380 m on Fig. 5) until the topography was filled (Fig. 11c). In Quebrada de Trancas at 380 m, there is a shift from a parasequence set dominated by river processes (i.e., delta-front; from 188 to 280 m) to a wave-dominated parasequence set (i.e., foreshore-shoreface and offshore; from 280 to 624 m). Such a switch of processes (i.e., from the river- to wave-dominated) and renewal of sedimentation in Sierra de Cajas (*Kainella andina* biozone) suggest that the previously created topographic high, preventing wave processes to occur in Quebrada de Trancas is not active anymore. This is probably due to the infill of the topographic low by DF1 and DF2 deposits (Fig. 11b, c).

Thus, wave propagation was no longer blocked and wave-dominated settings were established (Fig. 11c).

Previously, it was proposed that this sedimentary basin had an east-to-west prograding trend (e.g., Astini 2003). However, this trend is not consistent with the sandstone deltaic lobe progradation (Fig. 10a, b, d), the geometrical organization of the stratigraphic units (Fig. 11) or the paleocurrent indicators (i.e., flute casts, gutter casts; see Fig. 9d, f), which all point to a south-to-north trend of deposition. Therefore, it is more consistent with the northward orientations proposed by Buatois and Mángano (2003) and Buatois et al. (2006).

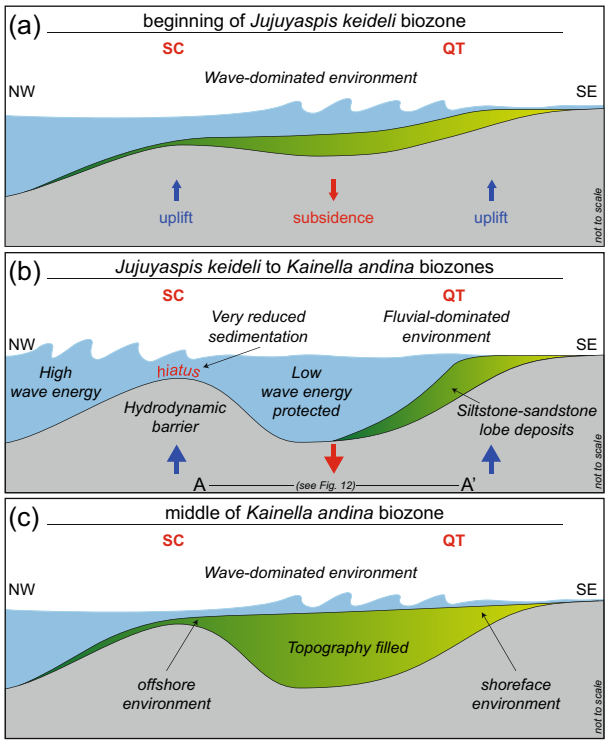

Fig. 11 Southeast-northwest cross-sections between Sierra de Cajas (SC) and Quebrada de Trancas (QT) showing the evolution at different time frames during the early Tremadocian. **a** Initiation of deformation during the Cambrian-Ordovician transition. The deformation started inducing both local uplift (blue arrow) and subsidence (red arrow). Physiographical changes were still weak, allowing the establishment of open wave-dominated environments during the transgressive phase at the beginning of the *Jujuyaspis keideli* biozones. **b** The intensity of deformation increased, accentuating local uplift and subsidence, and forming a high relief in SC. The latter acted as a hydrodynamic barrier dissipating incoming wave energy that winnowed sediment in this locality. Thus, SC created protected environments southward, allowing the development of the lobe-shaped deltaic deposits in QT from *Jujuyaspis keideli* to *Kainella andina* biozones. A–A' transect refer to Fig. 12. **c** The physiography remained as it was in **b** and the distal to proximal delta-front progressively filled the inherited topography up to SC. Once the topography was filled, open wave-dominated environments set up from the middle of *Kainella andina* biozone. Yellowish color corresponds to sandstone-dominated deposits, whereas the greenish one corresponds to mudstone-dominated deposits

Sequence stratigraphy

Interpretation in terms of stratigraphic sequences is proposed for the four stratigraphic sections. Identification of long-, medium, and short-term sequences is possible by the facies-zone description established previously (Fig. 5). Short-term sequences are the smallest sequences described in this study (Fig. 5). They vary between ~ 10 and ~ 100 m thick, reflecting the lithological change from siltstone- to sandstone-dominated intervals. Medium-term sequences of ~ 30 to ~ 160 m thick are composed of two small-scale sequences defined by a lower siltstone-dominated short-term sequence and an upper sandstone-dominated short-term sequence (Fig. 5). Long-term sequences consist of two medium-scale sequences and show a thickness of ~ 80 to ~ 180 m. They reflect the transition from siltstone- to sandstone-dominated medium-term sequences (Fig. 5).

The FAD of *Neoparabolina frequens argentina* corresponds to the FAD of *Cordylordus proavus* (conodont biozone; Shergold 1988; Waisfeld and Vaccari 2008 and references therein). According to Ogg et al. (2016a, b), the FAD of *Cordylordus proavus* was estimated at ~ 486.7 Ma. The limit between *Kainella meridionalis* and *Kaninella teiichii* biozones corresponds to the limit between Tr1 and Tr2, estimated at ~ 480.2 Ma (Ogg et al. 2016a, b). From the FAD of *Neoparabolina frequens argentina* to the Tr1–Tr2 boundary, six long-term sequences are recognized, encompassing an estimated duration of ~ 6.4 myr. The proposed duration for a long-term sequence is therefore of ~ 1.28 myr. According to the long-term sequence duration, this can be considered as a third-order cycle (e.g., Strasser et al. 2006). Thus, medium-term and short-term sequences have a respective duration of ~ 642 kyr and ~ 301 kyr. Medium-term sequences would correspond to the fourth-order cycle, and short-term sequences can reflect the long-term of the eccentricity cycle (Strasser et al. 2006). Nevertheless, because unconformities of unknown duration are recognized in the stratigraphic succession, caution should be exercised while considering these estimated durations.

Geodynamic implications

Several authors have characterized the upper Cambrian—Lower Ordovician strata from the Cordillera Oriental as recording long-term relative sea-level fluctuations devoid of tectonically induced deformation during the deposition (Moya 1988, 1997; Astini 2003, 2008; Buatois and Mángano

2003; Buatois et al. 2003; Mángano and Buatois 2004; Buatois et al. 2006). The tectonic setting changed with the development of a volcanic arc to the west and a retro-arc basin in the earliest Ordovician (Pankhurst et al 1998; Bahlburg 1998; Zimmermann and Bahlburg 2003; Zimmermann 2011). This study suggests that major changes in stratigraphic architecture occurred in response to modifications of the basin physiography (Figs. 5, 11 and 12), likely during the Cambrian—Ordovician transition (Fig. 5). As shown previously, the Cambrian strata were uplifted at Sierra de Cajas and Angosto del Moreno, and tilted at Quebrada de Trancas (Fig. 12). These deformations were responsible for changes in hydrodynamic processes and contributed to the development of extensive wave ravinement surfaces and sedimentary hiatus (Figs. 5, 10 and 11). On the west/south-west margin of the basin, the Puna-Famatinian volcanic arc (Fig. 12) developed at the beginning of the Early Ordovician, as a result of northeast-directed subduction, leading to the formation of a retro-arc basin to the east/north-east in the Cordillera Oriental and northward in Bolivia (Fig. 12; Bahlburg 1991; Pankhurst et al. 1998; Zimmermann and Bahlburg 2003; Zimmermann et al. 2010, 2014; Zimmermann 2011). Evidence of the arc activity is first recorded in Puna by felsic volcanic rocks from the volcanoclastic Vicuñas Formation and other Tremadocian successions (Moya et al. 1993; Zimmermann and Bahlburg 2003). Even if the trilobite fauna found in the Vicuñas Formation is suggestive of an Ordovician age, some upper Cambrian fauna was also discovered near the base of the deposits (Moya et al. 1993). According to Pankhurst et al. (1998), the associated magmatic activity commenced prior to the full development of the volcanic arc during the late Cambrian. Development of the volcanic arc drove large-scale deformation of the lithosphere in the retro-arc domain, leading to subsidence in the foredeep area and uplift in the forebuldge (e.g., Jordan 1995). This mechanism very likely explains (1) the forced regression in Sierra de Cajas, as well as the presence of a topographic barrier protecting the southern part of the study area (Figs. 11b and 12); and, (2) the extensive wave ravinement surfaces formed during the early Tr1 over uplifted surfaces at Angosto del Moreno and Quebrada de Trancas.

Southward, at Sierra de Famatina (Fig. 1), the Volcancito Formation has yielded a similar trilobite fauna (*Neoparabolina frequens argentina* and *Jujuyaspis keideli* biozones), allowing stratigraphic comparison with the present studied area (Tortello and Esteban 2007). A similar environmental deepening-upward trend is recorded, but in the Volcancito Formation the transgression occurred within the *Neoparabolina frequens argentina* biozone and not at the beginning of the *Jujuyaspis keideli* biozone. According to Rapela et al (2018), the onset of the magmatic activity in both the Puna and the Sierra de Famatina was synchronous, and coincided with the Cambrian-Ordovician transition. This suggests that deformation resulting in the deepening trend could reflect the onset of the foredeep subsidence. In the Sierra de Mojotoro (Fig. 2), no *Neoparabolina frequens argentina* was found (Harrington and Leanza 1957; Balseiro and Waisfeld 2013; Barrientos Ginés et al. 2018), suggesting that there are no coeval strata of the Lampazar Formation and the Casa Colorada Member further south. Indeed, the basal conglomeratic Pedrera Formation (Moya 1998; coeval to the Pupusa Formation and Alfarcito Member) rests directly on top of the Mesón Group. The absence of upper Cambrian deposits yielding *Neoparabolina frequens argentina* may either reflect non-deposition from emergence in the Sierra de Mojotoro (Fig. 2) or erosion following tectonic uplift at the Cambrian–Ordovician transition. The conglomeratic units in the Salta area may be coeval with the breccias (FS4) of Quebrada de Trancas, but further investigation should be undertaken to assess the provenance of this conglomeratic unit. Other sections exist in the Cordillera Oriental encompassing the same stratigraphic interval (e.g., Astini 2003, Benedetto 2007; Esteban and Tortello 2007; Esteban and Tortello 2009); however, the published stratigraphic intervals are lack of sedimentologic details or are poorly constrained, making comparisons difficult with the present study.

In summary, this study highlights a previously unrecognized episode of basin deformation around the Cambrian-Ordovician transition (Fig. 12). This stratigraphic unconformity was likely concomitant with the onset of the retro-arc basin in the Cordillera Oriental that probably occurred earlier in the western/southwestern foredeep area in the vicinity of the volcanic arc (Fig. 12). Nevertheless, in the foredeep area of the Puna, a strong deepening is expected during the late Cambrian as recognized in the Volcancito Formation further south, in Sierra de Famatina (Tortello and Esteban 2007). As the foredeep is characterized by strong subsidence rates and deepening trends, no wave ravinement is suspected. Further, detailed sedimentologic studies are also required in this area to constrain the evolution and the record of the deformation created by the Puna-Famatinian arc.

Conclusions

The studied upper Cambrian-Lower Ordovician stratigraphic interval of Cordillera Oriental in northwest Argentina was previously interpreted as a sedimentary succession only recording long-term sea-level fluctuations of a different order, with an east-to-west depositional trend, devoid of tectonically induced deformation. This first integrated study highlights a more complex history. Main points are summarized hereafter:

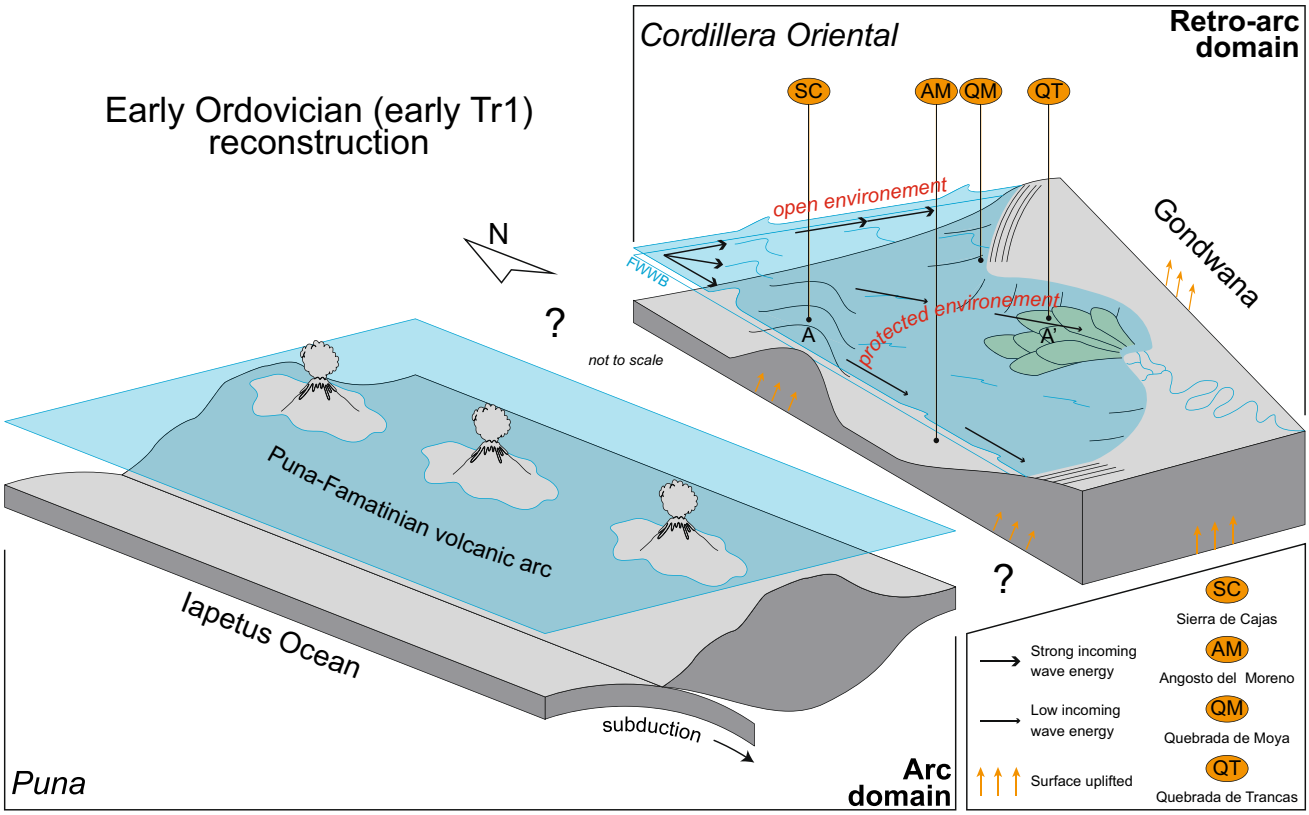

Fig. 12 Proposed reconstruction of the studied area during the Early Ordovician *Jujuyasips keideli* biozone. The basin in opened towards the north, while the physiography of the basin in the retro-arc domain is driven by the onset of the Puna-Famatinian arc to the west

- Ranging from late Cambrian (Age 10; *Neoparabolina frequens argentina* biozone) to Early Ordovician (Tr1; *Jujuyaspis keideli, Kainella andina, Kainella meridionalis* biozones), four main facies assemblages were described: estuarine, foreshore-shoreface, delta-front, and offshore. Correlation was possible due to the recognition of key trilobite taxa. The stacking patterns of facies assemblages suggest five third-order sequences of ~ 1.28 myr in duration.
- Basin physiographic changes are highlighted by (1) extensive wave ravinement surfaces at the Cambrian-Ordovician transition (at Quebrada de Trancas and Angosto del Moreno), (2) an unconformity between the Pico de Halcón (Cambrian) and Alfarcito (Ordovician) members, (3) a diachronic southward transgression, and (4) a change in coastal processes from river-dominated to wave-dominated across the *Jujuyaspis keideli* to *Kainella andina* biozones.
- The development of the Puna-Famatinian volcanic arc is considered as the driver for the deformation occurring in the basin. The deformation was associated with a change in basin style, from extensional to retro-arc. Therefore, this study confirms the proposal of Bahlburg and Hervé (1997) regarding tectonic disturbance present throughout the stratigraphic successions. This study highlights the complex stratigraphic evolution associated with the onset of a retro-arc basin in the forebuldge area.
- A revised lithostratigraphic framework is proposed, with newly formally defined formational names, assisting in the correlation between eastern (Quebrada de Trancas and Quebrada de Moya) and western (Sierra de Cajas and Angosto del Moreno) areas of the Cordillera Oriental.

Acknowledgements We are thankful to Compañía Minera Aguilar S.A, Florencia Califano, Fernando Hongn and Marissa Fabrezi for hosting us during fieldwork. Grateful considerations are given to the aboriginal communities of Casa Grande, Vizcarra and El Portillo de Aguilar, who allowed us to work in the area of Sierra de Cajas. M. Gabriela Mángano, Brian Pratt, Sebastián O. Verdecchia, and Blanca A. Toro are thanked for fruitful discussion. Romain Vaucher gives special thanks to Juan A. Moreno, Nicolás J. Cosentino and Cecilia Echegoyen for their *buena onda* during these years providing a good working atmosphere as well to Samantha Blandin, who followed him through this postdoctoral journey far away from our home. The manuscript has been improved due to constructive comments made by the reviewers Udo Zimmermann, María Cristina Moya and Martin Keller. Financial support for this study was provided by Consejo Nacional de Investigaciones Científicas y Técnicas (CONICET) Grant PIP 112-201201-00581, Agencia Nacional de Promoción Científica y Tecnológica (ANPCyT-FONCyT) PICT 2016-0588 and Global

Ambassador Incoming Program of the University of Saskatchewan. Field trips and fossil collections were made under permission of the Secretaría de Cultura de la Provincia de Jujuy (Res. 01390_SC/2015) and the Secretaría de Cultura, Ministerio de Cultura y Turismo de la Provincia de Salta (Disp. int. 010/2010 and 007/2014). This is a contribution to PUE 2016 (CICTERRA–CONICET).

Appendix 1: Proposed Stratigraphic Subdivision

The Guayoc Chico Group is redefined in this study and subdivided into four stratigraphic formations (see main text for details and Figs. 4 and 5 for correlation with other formational names). From base to top, these are: the Pardioc, Lampazar, Angosto del Moreno, and Pupusa formations. The Padrioc and the Lampazar formations were previously defined in the literature; however, the Angosto del Moreno and the Pupusa formations are newly introduced names in this study and are defined hereafter.

Angosto del Moreno formation

Name origin	*Angosto del Moreno* is the name of the locality where the formation is described.
Type area	Southeast of Salinas Grandes area, Province of Jujuy, Argentina.
Type section	Angosto del Moreno.
GPS points	Base 23°55′18.17″S 65°48′52.49″W.
	Top 23°55′19.18″S 65°48′47.05″W.
Facies	Greyish sandstone-dominated interval mostly displaying trough cross-stratification. Siltstone-dominated intervals are interbedded with hummocky cross-stratified sandstone.
Thickness	Maximum 120 m; minimum 60 m.
Boundaries	The base is placed where trough cross-stratified, medium-grained sandstone replaces a muddy siltstone-dominated interval of the Lampazar Formation. The upper boundary corresponds to the base of a muddy siltstone-dominated interval of the Pupusa Formation.
Fossils	Neoparabolina frequens argentina (Kayser 1876); Beltella ulrichi (Kayser 1897).
Age	Late Cambrian; Furongian; late Age 10.
Note	The wave ravinement surface eroding the Angosto del Moreno Formation occurring in the Angosto del Moreno is responsible for the thickness variation (see Fig. 10c).

Pupusa formation

Name origin	*Pupusa* is the vernacular name of a plant growing in the Andes used by native people as an infusion for helping with the altitude sickness.
Type area	Southeast of Salinas Grandes area, Province of Jujuy, Argentina.
Type section	Angosto del Moreno.
GPS points	Base 23°54′51.96″S 65°49′0.46″W.
	Top 23°54′51.49″S 65°48′48.77″W.
Facies	Greenish siltstone-dominated package with interbedded trough cross-stratified sandstone, hummocky cross-stratified sandstone and mudstone. In the upper part of this interval, interbedded trough cross-stratified sandstone and shell beds become increasingly common.
Thickness	maximum 160 m minimum 100 m.
Boundaries	The base corresponds to the transition from a trough cross-stratified sandstone-dominated interval of the Angosto del Moreno Formation to a siltstone-dominated interval. The Pupusa Formation ends with the Tumbaya Unconformity mantled by the siltstone-dominated package of the Acoite Formation (Middle Ordovician; Floian - Dapingian)
Fossils	*Jujuyaspis keideli* (Kobayashi 1936); *Leiostegium douglasi* (Harrigton 1937); *Saltaspis steinmanni* (Koabayashi 1936); *Hapalopleura acantha* (Malanca & Brandán 2000); *Parabollinella argentinensis* (Kobayashi 1936); *Onychopyge* sp, *Kainella morena* (Vaccari & Waisfeld 2010); *Kvania azulpampensis azulpampensis* (Benedetto 2007); *K. azulpampensis dichotoma* (Benedetto 2007); *Gondwanorthis calderensis alternata* (Benedetto and Muñoz 2017); *Chaniella pascuali* (Benedetto 2009).
Age	Early Ordovician; Tremadocian; early Tr1.
Note	The wave-ravinement surface eroding the Angosto del Moreno Formation at Angosto del Moreno is responsible for the thickness variation, since the Pupusa Formation fills the created depression (see Fig. 10c).

References

Aceñolaza FG, Miller H, Toselli AJ (1988) The Puncoviscana Formation (late Precambrian—early Cambrian). Sedimentology, tectonometamorphic history and age of the oldest rocks of nw argentina. In: Bahlburg H, Breitkreuz C, Giese P (eds) The Southern Central Andes: contributions to structure and evolution of an active continental margin. Springer, Berlin, Heidelberg, pp 25–37. https://doi.org/10.1007/BFb0045172

Albanesi GL, Giuliano ME, Pacheco F, Ortega G, Monaldi CR (2015) Conodonts from the Cambrian-Ordovician boundary in the Cordillera Oriental. NW Argentina Stratigr 12:237–256

Aris MJ, Corronca JA, Quinteros S, Pardo PL (2017) A new marrellomorph euarthropod from the Early Ordovician of Argentina. Acta Palaeontol Pol 62:1–8

Astini RA (2003) The Ordovician Proto-Andean basins. In: Benedetto JL (ed) Ordovician fossils of Argentina. Universidad Nacional de Córdoba, Secretaría de Ciencia y Tecnología, pp 1–74

Astini RA (2005) Las sedimentitas que apoyan en no concordancia sobre el" granito rojo" en el Angosto de la Quesera (Cordillera Oriental, Salta): una revisión crítica a más de 60 años de los trabajos pioneros de. J Keidel Rev Asoc Geol Argentina 60:513–523

Astini RA (2008) Sedimentación, facies, discordancias y evolución paleoambiental durante el Cambro-Ordovícico Geología y Recursos Naturales de la provincia de Jujuy, Relatorio del XVII Congreso Geológico Argentino, Jujuy, pp 50–73

Augustsson C et al (2011) Detrital quartz and Zircon combined: the production of mature sand with short transportation paths along the Cambrian West Gondwana margin, Northwestern Argentina. J Sediment Res 81:284–298. https://doi.org/10.2110/jsr.2011.23

Bahlburg H (1991) The Ordovician back-arc to foreland successor basin in the Argentinian—Chilean Puna: Tectono-sedimentary trends and sea-level changes. In: Macdonald DI (ed) Sedimentation, tectonics and eustasy, vol 12. Special Publication of the International Association of Sedimentology, pp 465–484. https://doi.org/10.1002/9781444303896.ch25

Bahlburg H (1998) The geochemistry and provenance of Ordovician turbidites in the Argentine Puna. In: Pankhurst RJ, Rapela CW (eds) The Proto-Andean Margin of Gondwana. Geol Soc Lond Spec Publ, vol 142, pp 127–142

Bahlburg H, Furlong KP (1996) Lithospheric modeling of the Ordovician foreland basin in the Puna of northwestern Argentina: on the influence of arc loading on foreland basin formation. Tectonophysics 259:245–258. https://doi.org/10.1016/0040-1951(95)00129-8

Bahlburg H, Hervé F (1997) Geodynamic evolution and tectonostratigraphic terranes of northwestern Argentina and northern Chile. GSA Bull 109:869–884. https://doi.org/10.1130/0016-7606(1997)109%3c0869:GEATTO%3e2.3.CO;2

Bahlburg H, Moya MC, Zeil W (1994) Geodynamic Evolution of the Early Palaeozoic Continental Margin Of Gondwana In the Southern Central Andes of Northwestern Argentina and Northern Chile. In: Reutter K-J, Scheuber E, Wigger PJ (eds) Tectonics of the Southern Central Andes: structure and evolution of an active continental margin. Springer, Berlin, Heidelberg, pp 293–302. https://doi.org/10.1007/978-3-642-77353-2_21

Bahlburg H, Vervoort JD, Du Frane SA, Bock B, Augustsson C, Reimann C (2009) Timing of crust formation and recycling in accretionary orogens: Insights learned from the western margin of South America. Earth Sci Rev 97:215–241. https://doi.org/10.1016/j.earscirev.2009.10.006

Balseiro D, Waisfeld B, Vaccari E (2011) Paleoecological dynamics of Furongian (Late Cambrian) trilobite-dominated communities from northwestern Argentina. Palaios 26:484–499. https://doi.org/10.2110/palo.2010.p10-152r

Balseiro D, Waisfeld BG (2013) Ecological instability in Upper Cambrian-Lower Ordovician trilobite communities from Northwestern Argentina. Palaeogeogr Palaeoclimatol Palaeoecol 370:64–76. https://doi.org/10.1016/j.palaeo.2012.11.019

Barrientos Ginés AV, Aparicio González P, Bercheñi VA, Moya MC (2018) Estratigrafía y sedimentología de las unidades ordovícicas del tramo central de la sierra de Mojotoro Cordillera Oriental, Noroeste Argentino. Rev Asoc Geol Argentina 75:609–625

Beckvar N, Kidwell SM (1988) Hiatal shell concentrations, sequence analysis, and sealevel history of a Pleistocene coastal alluvial fan Punta Chueca, Sonora. Lethaia 21:257–270. https://doi.org/10.1111/j.1502-3931.1988.tb02078.x

Beji S, Battjes JA (1993) Experimental investigation of wave propagation over a bar. Coast Eng 19:151–162. https://doi.org/10.1016/0378-3839(93)90022-Z

Benedetto JL (2007) New Upper Cambrian-Tremadoc rhynchonelliformean brachiopods from northwestern Argentina: evolutionary trends and early diversification of plectorthoideans in the Andean Gondwana. J Paleontol 81:261–285. https://doi.org/10.1666/0022-3360(2007)81[261:NUCRBF]2.0.CO;2

Benedetto JL, Carrasco PA (2002) Tremadoc (earliest Ordovician) brachiopods from Purmamarca and the Sierra de Mojotoro, Cordillera Oriental of northwestern Argentina. Geobios 35:647–661. https://doi.org/10.1016/S0016-6995(02)00079-7

Bhattacharya JP, Giosan L (2003) Wave-influenced deltas: geomorphological implications for facies reconstruction. Sedimentology 50:187–210. https://doi.org/10.1046/j.1365-3091.2003.00545.x

Bhattacharya JP, MacEachern JA (2009) Hyperpycnal rivers and prodeltaic shelves in the cretaceous seaway of North America. J Sediment Res 79:184–209. https://doi.org/10.2110/jsr.2009.026

Bhattacharya JP, Posamentier HW, Walker RG (2006) Deltas. In: Facies Models Revisited, vol 84. SEPM Society for Sedimentary Geology. https://doi.org/10.2110/pec.06.84.0237

Bock B, Bahlburg H, Wörner G, Zimmermann U (2000) Tracing crustal evolution in the Southern Central Andes from late Precambrian to Permian with geochemical and Nd and Pb isotope data. J Geol 108:515–535. https://doi.org/10.1086/314422

Botquelen A, Loi A, Gourvennec R, Leone F, Dabard M-P (2004) Formation et signification paléo-environnementale des concentrations coquillières: exemples de l'Ordovicien de Sardaigne et du Dévonien du Massif Armoricain. Compt Rend Palevol 3:353–360. https://doi.org/10.1016/j.crpv.2004.06.003

Buatois LA, Mangano MG, Moya MC (2000) Incisión de valles estuarinos en el Cámbrico Tardío del noroeste argentino y la problemática del límite entre los grupos Mesón y Santa Victoria Segundo Congreso Latinoamericano de Sedimentología Resúmenes. Mar del Plata 2000:55

Buatois LA, Mángano MG (2003) Sedimentary facies, depositional evolution of the Upper Cambrian-Lower Ordovician Santa Rosita formation in northwest Argentina. J South Am Earth Sci 16:343–363. https://doi.org/10.1016/S0895-9811(03)00097-X

Buatois LA, Mángano MG (2005) Discussion and reply: the Cambrian system in Northwestern Argentina: stratigraphical and palaeontological framework. Discuss Geol Acta 3:65–72

Buatois LA, Moya MC, Mángano MG, Malanca S (2003) Paleoenvironmental and sequence stratigraphic framework of the Cambrian-Ordovician transition in the Angosto del Moreno area, northwest Argentina. Int Symp Ordovician Syst 2003:397–401

Buatois LA, Santiago N, Herrera M, Plink-Björklund P, Steel R, Espin M, Parra K (2012) Sedimentological and ichnological signatures of changes in wave, river and tidal influence along a Neogene tropical deltaic shoreline. Sedimentology 59:1568–1612. https://doi.org/10.1111/j.1365-3091.2011.01317.x

Buatois LA, Zeballo FJ, Albanesi GL, Ortega G, Vaccari E, Mángano MG (2006) Depositional environments and stratigraphy of the Upper Cambrian-Lower Ordovician Santa Rosita formation at the Alfarcito area, Cordillera Oriental, Argentina: integration of biostratigraphic data within a sequence stratigraphic framework. Latin Am J Sedimentol Basin Anal 13:65–95

Casquet C et al (2018) Review of the Cambrian Pampean orogeny of Argentina; a displaced orogen formerly attached to the Saldania Belt of South Africa? Earth Sci Rev 177:209–225. https://doi.org/10.1016/j.earscirev.2017.11.013

Casquet C et al (2012) A history of Proterozoic terranes in southern South America: from Rodinia to Gondwana. Geosci Front 3:137–145. https://doi.org/10.1016/j.gsf.2011.11.004

Cattaneo A, Steel RJ (2003) Transgressive deposits: a review of their variability. Earth Sci Rev 62:187–228. https://doi.org/10.1016/S0012-8252(02)00134-4

Clemens K (1993) Sedimentologia, proveniencia y desarrollo geotect6nico del Sistema de Famatina en el Noroeste de Argentina durante el Paleozoico inferior. XII Congreso Geológico Argentino y II Congreso de Exploración de Hidrocarburos Actas Mendoza 1:310–320

Clifton HE (2006) A re-examination of facies models for clastic shorelines. In: Posamentier HW, Walker RG (eds) Facies Model Revisited, vol 84. SEPM, Special Publication, pp 293–337

Coates L, MacEachern JA (2007) The ichnological signatures of river- and wave-dominated delta complexes: differentiating deltaic from non-deltaic shallow marine successions, Lower Cretaceous Viking Formation and Upper Cretaceous Dunvegan Formation, west-central Alberta. In: MacEachern JA, Bann KL, Gingras MK, Pemberton SG (eds) Applied Ichnology: SEPM, Short Course Notes 52, pp 227–254

Collinson JD, Mountney N, Thompson DB (2006) Sedimentary structures (3rd ed). Terra, Harpenden, Hert, England

Dalrymple RW, Choi K (2007) Morphologic and facies trends through the fluvial-marine transition in tide-dominated depositional systems: a schematic framework for environmental and sequence-stratigraphic interpretation. Earth Sci Rev 81:135–174

Dalziel IWD (1997) Overview: neoproterozoic-paleozoic geography and tectonics: review, hypothesis, environmental speculation. Geol Soc Am Bull 109:16–42. https://doi.org/10.1130/0016-7606(1997)109%3c0016:onpgat%3e2.3.co;2

Dunham RJ (1970) Keystone Vugs in carbonate beach deposits. AAPG Bull 54:845

Duperron M, Scasso RA (2020) Paleoenvironmental significance of microbial mat-related structures and ichnofaunas in an Ordovician mixed-energy estuary Áspero Formation of Santa Victoria Group, northwestern Argentina. J Sediment Res 90:364–388. https://doi.org/10.2110/jsr.2020.17

Egenhoff SO (2007) Life and death of a Cambrian-Ordovician basin: an Andean three-act play featuring Gondwana and the Arequipa-Antofalla terrane. Geol Soc Am Spec Papers 423:511–524

Escayola MP, van Staal CR, Davis WJ (2011) The age and tectonic setting of the Puncoviscana formation in northwestern Argentina: an accretionary complex related to Early Cambrian closure of the Puncoviscana Ocean and accretion of the Arequipa-Antofalla block. J Soc Am Earth Sci 32:438–459. https://doi.org/10.1016/j.jsames.2011.04.013

Esteban SB, Tortello MF (2007) Latest Cambrian sedimentary settings and trilobite faunas from the western Cordillera Oriental, Argentina. Memoirs Assoc Austr Palaeontol 34:431–460

Esteban SB, Tortello MF (2009) Sedimentología y paleontología de la Formación Sant a Rosita (Miembros Tilcara y Casa Colorada, Cámbrico Tardío) en la región de Iruya, provincia de Salta. Acta Geol lilloana 2009:129–153

Fernández R, Guerrero C, Manca N (1982) El límite Cámbro-Ordovícico en el tramo medio y superior de la quebrada de Humahuaca, Provincia de Jujuy, Argentina 5to Congreso Latinoamericano de Geología, Actas. Buenos Aires 1:3–22

Gohrbandt KHA (1992) Paleozoic paleogeographic and depositional developments on the central proto-Pacific margin of Gondwana: their importance to hydrocarbon accumulation. J Soc Am Earth Sci 6:267–287. https://doi.org/10.1016/0895-9811(92)90046-2

Gugliotta M, Saito Y, Nguyen VL, Ta TKO, Tamura T, Fukuda S (2018) Tide- and river-generated mud pebbles from the fluvial to marine transition zone of the Mekong River Delta, Vietnam. J Sediment Res 88:981–990. https://doi.org/10.2110/jsr.2018.54

Hampson GJ, Storms JEA (2003) Geomorphological and sequence stratigraphic variability in wave-dominated, shoreface-shelf parasequences. Sedimentology 50:667–701. https://doi.org/10.1046/j.1365-3091.2003.00570.x

Harrington HJ (1937) On some Ordovician fossils from Northern Argentina. Geol Mag 74:97–124. https://doi.org/10.1017/S0016756800088592

Harrington HJ (1957) Ordovician Formations of Argentina. In: Harrington HJ, Leanza AF (eds) Ordovician trilobites of Argentina, vol 1. University of Kansas Special Publication, pp 1–59

Harrington HJ, Leanza AF (1957) Ordovician fossils of Argentina. University of Kansas Press

Heward AP (1981) A review of wave-dominated clastic shoreline deposits. Earth Sci Rev 17:223–276. https://doi.org/10.1016/0012-8252(81)90022-2

Hwang I-G, Heller PL (2002) Anatomy of a transgressive lag: Panther Tongue Sandstone, Star Point Formation, central Utah. Sedimentology 49:977–999. https://doi.org/10.1046/j.1365-3091.2002.00486.x

Jordan TE (1995) Retroarc foreland and related basins. In: Busby CJ, Ingersoll RV (eds) Tectonics of sedimentary basins. Blackwell Science, Oxford, pp 331–362

Kleine T, Mezger K, Zimmermann U, Münker C, Bahlburg H (2004) Crustal evolution along the early Ordovician Proto-Andean Margin of Gondwana: trace element and isotope evidence from the Complejo Igneo Pocitos (Northwest Argentina). J Geol 112:503–520. https://doi.org/10.1086/422663

Kley J, Monaldi CR, Salfity JA (1999) Along-strike segmentation of the Andean foreland: causes and consequences. Tectonophysics 301:75–94. https://doi.org/10.1016/S0040-1951(98)90223-2

Lokier SW, Al Junaibi M (2016) The petrographic description of carbonate facies: are we all speaking the same language? Sedimentology 63:1843–1885. https://doi.org/10.1111/sed.12293

MacEachern JA, Bann KL, Bhattacharya JP, Howell CD, Jr (2005) Ichnology of deltas: organism responses to the dynamic interplay of rivers, waves, storms, and tides. In: Bhattacharya JP, Giosan L (eds) River deltas—concepts, models, and examples: SEPM, Special Publication vol 83, pp 49–85

Malanca S, Brandán EM (2000) Nuevos Orometopidae (Asaphida, Trilobita) de la Formación Saladillo, Tremadoc Temprano de la Cordillera Oriental argentina XIV Congreso Geológico Boliviano, La Paz Memorias, pp 131–135

Mángano MG, Buatois LA (1996) Shallow marine event sedimentation in a volcanic arc-related setting: the Ordovician Suri Formation, Famatina Range, northwest Argentina. Sed Geol 105:63–90

Mángano MG, Buatois LA (1997) Slope-apron deposition in an Ordovician arc-related setting: the Vuelta de Las Tolas Member (Suri Formation), Famatina Basin, northwest Argentina. Sed Geol 109:155–180

Mángano M, Buatois L (2003) Trace fossils. In: Benedetto J (ed) Ordovician fossils of Argentina. Universidad Nacional de Córdoba, Secretaría de Ciencia y Tecnología, pp 507–553

Mángano MG, Buatois LA (2004) Integración de estratigrafía secuencial, sedimentología e icnología para un análisis cronoestratigráfico del Paleozoico inferior del noroeste argentino. Rev Asoc Geol Argentina 59:273–280

Mángano MG, Buatois LA, Muñiz Guinea F (2005) Ichnology of the Alfarcito Member (Santa Rosita Formation) of northwestern Argentina: animal-substrate interactions in a lower Paleozoic wave-dominated shallow sea. Ameghiniana 42:28

Mannheim R (1993) Genesis de las volcanitas eopaleozoicas de! Sistema de! Famatina, noroeste de Argentina. XII Congreso Geológico Argentino y II Congreso de Exploración de Hidrocarburos Actass, Mendoza 4:47–155

Meroi Arcerito FR, Waisfeld BG, Vaccari NE, Muñoz DF (2018) High resolution trilobite biostratigraphy for the early Late Tremadocian (Tr2) interval (Early Ordovician) Santa Rosita formation. Argentine Cordillera Oriental Ameghiniana 55(531–553):523

Mon R, Hongn F (1996) Estructura del basamento proterozoico y paleozoico inferior del norte argentino. Rev Asoc Geol Argentina 51:3–14

Mon R, Salfity JA (1995) Tectonic evolution of the Andes of northern Argentina. In: Tankard AJ, Suárez Soruco R, Welsink HJ (eds) Petroleum Basins of South America. Am. Assoc. Petrol. Geol., Tulsa, Oklahoma, pp 269-283

Moya M (1998) El Paleozoico inferior en la sierra de Mojotoro, Salta-Jujuy. Rev Asoc Geol Argentina 53:219–238

Moya MC (1988) Lower Ordovician in the southern part of the Argentine eastern Cordillera. In: Bahlburg H, Breitkreuz C, Giese P (eds) The Southern Central Andes: contributions to structure and evolution of an active continental Margin. Springer, Berlin, Heidelberg, pp 55–69. https://doi.org/10.1007/BFb0045174

Moya MC La fase Tumbaya (Ordovícico Inferior) en los Andes del norte argentino. In: VIII Congreso Geológico Chileno, 1997. pp 185–189

Moya MC, Malanca S, Hongn FD, Bahlburg H (1993) El Tremadoc temprano en la Puna occidental argentina. XII Congreso Geológico Argentino y II Congreso de Exploración de Hidrocarburos Actas 2:20–30

Moya MC, Malanca S, Monteros JA, Albanesi GL, Ortega G, Buatois LA (2003) Late Cambrian–Tremadocian faunas and events from the Angosto del Moreno section, Eastern Cordillera, Argentina. In: Albanesi GL, Beresi MS, Peralta SH (eds) Ordovician from the Andes, vol 17. Serie de Correlación Geológica, pp 439–444

Moya MC, Monteros JA (2000) El Angosto del Moreno (Cordillera Oriental argentina), un área clave para analizar el límite Cámbrico–Ordovícico y la Discordancia Iruya. XIV Congreso Geológico Boliviano, La Paz Memorias, pp 142–147

Muñoz DF, Benedetto JL (2016) The eoorthid brachiopod Apheoorthina in the Lower Ordovician of NW Argentina and the dispersal pathways along western Gondwana. Acta Palaeontol Pol 61:633–644

Muñoz DF, Mángano MG, Buatois LA (2018) *Gyrophyllites cristinae* isp. nov. from Lower Ordovician Shallow-Marine Deposits of Northwest Argentina. Ichnos 2018:1–13. https://doi.org/10.1080/10420940.2018.1538983

Niemeyer H, Götze J, Sanhueza M, Portilla C (2018) The Ordovician magmatic arc in the northern Chile-Argentina Andes between 21° and 26° south latitude. J S Am Earth Sci 81:204–214. https://doi.org/10.1016/j.jsames.2017.11.016

Ogg JG, Ogg GM, Gradstein FM (2016a) 5—Cambrian. In: Ogg JG, Ogg GM, Gradstein FM (eds) A concise geologic time scale. Elsevier, Berlin, pp 41–55. https://doi.org/10.1016/B978-0-444-59467-9.00005-4

Ogg JG, Ogg GM, Gradstein FM (2016b) 6 - Ordovician. In: Ogg JG, Ogg GM, Gradstein FM (eds) A concise geologic time scale. Elsevier, Berlin, pp 57–69. https://doi.org/10.1016/B978-0-444-59467-9.00006-6

Olariu C, Bhattacharya JP (2006) Terminal distributary channels and delta front architecture of river-dominated delta systems. J Sediment Res 76:212–233. https://doi.org/10.2110/jsr.2006.026

Omarini RH, Sureda RJ, Götze H-J, Seilacher A, Pflüger F (1999) Puncoviscana folded belt in northwestern Argentina: testimony of Late Proterozoic Rodinia fragmentation and pre-Gondwana collisional episodes. Int J Earth Sci 88:76–97. https://doi.org/10.1007/s005310050247

Orton GJ, Reading HG (1993) Variability of deltaic processes in terms of sediment supply, with particular emphasis on grain size. Sedimentology 40:475–512. https://doi.org/10.1111/j.1365-3091.1993.tb01347.x

Pankhurst RJ, Rapela CW (1998) The proto-Andean margin of Gondwana: an introduction. Geol Soc Lond Spec Publ 142:1–9. https://doi.org/10.1144/gsl.sp.1998.142.01.01

Pankhurst RJ, Rapela CW, Saavedra J, Baldo E, Dahlquist J, Pascua I, Fanning CM (1998) The Famatinian magmatic arc in the central Sierras Pampeanas: an Early to Mid-Ordovician continental arc on the Gondwana margin. Geol Soc Lond Spec Publ 142:343–367. https://doi.org/10.1144/gsl.sp.1998.142.01.17

Perillo MM, Best J, Garcia MH (2014) A new phase diagram for combined-flow bedforms. J Sediment Res 84:301–313. https://doi.org/10.2110/jsr.2014.25

Plint AG (2010) Wave-and storm-dominated shoreline and shallow-marine systems. In: Dalrymple RW, James NP (eds) Facies models. 4 edn. Geol. Assoc. Canada, St John's, pp 167–200

Ramos VA (1973) Estructura de los primeros contrafuertes de la Puna salto-jujeña y sus manifestaciones volcánicas asociadas 5º Congreso Geológico Argentino. Carlos Paz Actas 4:159–202

Ramos VA (2018) Tectonic evolution of the Central Andes: From Terrane Accretion to Crustal Delamination. In: Zamora G, McClay KM, Ramos VA (eds) Petroleum basins and hydrocarbon potential of the Andes of Peru and Bolivia. AAPG Memoir 117, pp 1–34

Rapela CW et al (2018) A review of the Famatinian Ordovician magmatism in southern South America: evidence of lithosphere reworking and continental subduction in the early proto-Andean margin of Gondwana. Earth Sci Rev 187:259–285. https://doi.org/10.1016/j.earscirev.2018.10.006

Reading HG, Collinson JD (1996) Clastic coasts. In: Reading HG (ed) Sedimentary Environments: processes, facies and stratigraphy. Blackwell, Oxford, pp 154–231

Reineck H, Singh I (1980) Depositional sedimentary environments (with reference to Terrigenous Clastics). Spring, Germany, p 551

Ruiz Huidobro OJ (1975) El Paleozoico Inferior del centro y sur de Salta y su correlación con el Grupo Mesón 1er Congreso Argentino de Paleontología y Bioestratigrafía Actas. San Miguel de Tucumán 1:91–107

Salas MJ, Waisfeld BG, Muñoz DF (2018) Radiation, diversity and environmental expansion of Early Ordovician ostracods: a view from the Southern Hemisphere. Lethaia. https://doi.org/10.1111/let.12293

Sánchez MC, Salfity JA (1999) The Cambrian Mesón Group basin (NW Argentina): Stratigraphic and paleogeographic development. Acta Geol Hispanica 34:123–139

Serra F, Balseiro D, Waisfeld BG (2019) Diversity patterns in upper Cambrian to Lower Ordovician trilobite communities of northwestern Argentina. Palaeontology 62:677–695. https://doi.org/10.1111/pala.12424

Shergold JH (1988) Review of trilobite biofacies distributions at the Cambrian-Ordovician. Bound Geol Mag 125:363–380. https://doi.org/10.1017/S0016756800013030

Strasser A, Hilgen FJ, Heckel PH (2006) Cyclostratigraphy—concepts, definitions, and applications. Newsl Stratigr 42:75–114. https://doi.org/10.1127/0078-0421/2006/0042-0075

Toro BA, Herrera Sánchez NC (2019) Stratigraphical distribution of the Ordovician graptolite Azygograptus Nicholson & Lapworth

in the Central Andean Basin (northwestern Argentina and southern Bolivia). Comp Rend Palevol 18:493–507. https://doi.org/10.1016/j.crpv.2019.06.002

Tortello FM, Rábano I, Rao RI, Aceñolaza FG (1999) Los trilobites de la transición Cámbrico-Ordovicico en la quebrada Amarilla (Sierra de Cajas, Jujuy, Argentina). Boletín Geol Minero 110:555–572

Tortello MF, Esteban SB (2003) Trilobites del Cámbrico tardío de la Formación Lampazar (sierra de Cajas, Jujuy, Argentina). Impl Bioestrat Paleoambientales Ameghiniana 40:323–344

Tortello MF, Esteban SB (2007) Trilobites de la Formación Volcancito (Miembro Filo Azul, Cámbrico Tardío) del Sistema de Famatina La Rioja, Argentina. Aspectos Sistemát Paleoambientales 44:597–620

Turner JCM (1960) Estratigrafía de la Sierra de Santa Victoria y adyacencias. Boletín Acad Nacional Ciencias Córdoba 41:163–196

Turner JCM, Méndez V (1975) Geología del sector oriental de los departamentos de Santa Victoria e Iruya Provincia de Salta, República Argentina. Boletín Acad Nacional Ciencias Córdoba 51:11–24

Vaccari NE, Edgecombe GD, Escudero C (2004) Cambrian origins and affinities of an enigmatic fossil group of arthropods Nature 430:554–557 https://www.nature.com/nature/journal/v430/n6999/suppinfo/nature02705_S1.html

Vaccari NE, Waisfeld BG, Canelo HN, Smith L (2018) Trilobites from the Iscayachi Formation (Upper Cambrian–Lower Ordovician), Cordillera Oriental, South Bolivia. Biostratigraphic implications. In: Suárez Riglos M, Dalenz Farjat A, Pérez Leyton M (eds) Fósiles y Facies de Bolivia, pp 36–58

Vaccari NE, Waisfeld BG, Marengo LF, Smith L (2010) *Kainella* Walcott, 1925 (Trilobita, Ordovícico Temprano) en el noroeste de Argentina y sur de Bolivia. Import Bioestratigr Ameghiniana 47:293–305. https://doi.org/10.5710/AMGH.v47i3.5

Vaucher R, Pittet B, Hormière H, Martin ELO, Lefebvre B (2017) A wave-dominated, tide-modulated model for the Lower Ordovician of the Anti-Atlas, Morocco. Sedimentology 64:777–807. https://doi.org/10.1111/sed.12327

Vaucher R, Pittet B, Passot S, Grandjean P, Humbert T, Allemand P (2018) Bedforms in a tidally modulated ridge and runnel shoreface (Berck-Plage; North France): implications for the geological record. Earth Sci Bull 189:5

Waisfeld B, Vaccari E (2008) Bioestratigrafía de trilobites del Paleozoico inferior de la Cordillera Oriental. In: Coira B, Zappettini EO (eds) Geologia y Recursos Naturales de Jujuy Relatorio Del XVII Congreso Geológico Argentino. Asociación Geológica Argentina, Buenos Aires, Argentina, pp 119–127

Waisfeld BG, Balseiro D (2016) Decoupling of local and regional dominance in trilobite assemblages from northwestern Argentina: new insights into Cambro-Ordovician ecological changes. Lethaia 49:379–392. https://doi.org/10.1111/let.12153

Walker RG, James NP (1992) Facies models: response to sea level change. St. John's, Nfld. Geological Association of Canada

Zecchin M, Catuneanu O, Caffau M (2018) Wave-ravinement surfaces: classification and key characteristics. Earth Sci Rev. https://doi.org/10.1016/j.earscirev.2018.11.011

Zimmermann U (2011) From fore-arc to foreland: a cross-section of the Ordovician in the Central Andes. In: Gutiérrez-Marco J-C, Rábano I, García-Bellido D (eds) Ordovician of the World, vol 14. Cuadernos del Museo Geominero, Madrid, pp 667–674

Zimmermann U, Bahlburg H (2003) Provenance analysis and tectonic setting of the Ordovician clastic deposits in the southern Puna Basin, NW Argentina. Sedimentology 50:1079–1104. https://doi.org/10.1046/j.1365-3091.2003.00595.x

Zimmermann U, Bahlburg H, Mezger K, Berndt J, Kay SM (2014) Origin and age of ultramafic rocks and gabbros in the southern Puna of Argentina: an alleged Ordovician suture revisited. Int J Earth Sci 103:1023–1036. https://doi.org/10.1007/s00531-014-1020-y

Zimmermann U, Niemeyer H, Meffre S (2010) Revealing the continental margin of Gondwana: the Ordovician arc of the Cordón de Lila (northern Chile). Int J Earth Sci 99:39–56. https://doi.org/10.1007/s00531-009-0483-8